

Black-Box Testing of Deep Neural Networks through Test Case Diversity

Zohreh Aghababaeyan, Manel Abdellatif, Lionel Briand, Ramesh S, and Mojtaba Bagherzadeh

Abstract—Deep Neural Networks (DNNs) have been extensively used in many areas including image processing, medical diagnostics, and autonomous driving. However, DNNs can exhibit erroneous behaviours that may lead to critical errors, especially when used in safety-critical systems. Inspired by testing techniques for traditional software systems, researchers have proposed neuron coverage criteria, as an analogy to source code coverage, to guide the testing of DNN models. Despite very active research on DNN coverage, several recent studies have questioned the usefulness of such criteria in guiding DNN testing. Further, from a practical standpoint, these criteria are white-box as they require access to the internals or training data of DNN models, which is in many contexts not feasible or convenient.

In this paper, we investigate black-box input diversity metrics as an alternative to white-box coverage criteria. To this end, we first select and adapt three diversity metrics and study, in a controlled manner, their capacity to measure actual diversity in input sets. We then analyse their statistical association with fault detection using four datasets and five DNN models. We further compare diversity with state-of-the-art white-box coverage criteria.

Our experiments show that relying on the diversity of image features embedded in test input sets is a more reliable indicator than coverage criteria to effectively guide the testing of DNNs. Indeed, we found that one of our selected black-box diversity metrics far outperforms existing coverage criteria in terms of fault-revealing capability and computational time. Results also confirm the suspicions that state-of-the-art coverage metrics are not adequate to guide the construction of test input sets to detect as many faults as possible with natural inputs.

Index Terms—Deep Neural Network, Test, Diversity, Coverage, Faults.



1 INTRODUCTION

Over the last decade, Deep Neural Networks (DNNs) have achieved great performance in many domains, such as image processing [1], [2], medical diagnostics [3], [4], [5], speech recognition [6] and autonomous driving [7], [8].

Similar to traditional software components, DNN models often exhibit erroneous behaviours that may lead to potentially critical errors. Therefore, like traditional software, DNNs need to be tested effectively to ensure their reliability and safety.

In the software testing context, code coverage criteria (e.g., branch coverage, statement coverage) are used to guide the generation of test cases and assess the completeness of test suites [9]. While full coverage does not ensure functional correctness, high coverage increases stakeholders' confidence in the testing results since it triggers more code execution paths. Inspired by code coverage, several coverage criteria have been introduced to measure the adequacy of test data in the context of DNNs [10], [11], [12], [13], [14]. Neuron coverage measures the extent to which neurons in a DNN are activated based on certain input data. Intuitively, test inputs with a higher neuron coverage is desirable. However, reaching high neuron coverage with a few test inputs is usually easy to achieve [14], [15] and the usefulness of such coverage is therefore questionable. Furthermore, defining coverage in DNNs is not as straightforward as testing traditional software because, in the latter, the code logic is explicit whereas in DNNs, that logic is not explicitly represented. Although more sophisticated coverage criteria have been proposed, several articles have

criticised the use of such coverage to guide the testing of DNN models [16], [17], [18].

In fact, in traditional software systems, testers rely on coverage metrics as they assume that (1) inputs covering the same part of the source code are homogeneous, i.e. either all or none of these inputs trigger a failure, and (2) the inputs used in testing should be diverse to ensure high coverage [16]. However these assumptions break down in DNN testing as (1) as opposed to code coverage, neuron coverage does not necessarily fully exercise the implicit logic embedded in DNNs, (2) the homogeneity assumption is broken with adversarial inputs, and (3) increasing the diversity of inputs does not necessarily increase DNNs coverage [16]. Further, most coverage studies rely on adversarial inputs to validate their proposed criteria [12], [13], [14], [10], [11]. These inputs are, however, mostly unrealistic and are used to study the robustness of the DNN model instead of its accuracy. While state-of-the-art coverage criteria have been largely validated with artificial inputs generated based on adversarial methods, their claimed sensitivity to adversarial inputs does not necessarily mean that they relate to the fault detection capability of natural test input sets. This is confirmed by some studies [16], [18] that have failed to find a significant correlation between coverage and the number of misclassified inputs in a natural test inputs set, despite a positive correlation in the presence of adversarial test inputs. Consequently, coverage criteria may be ineffective in guiding DNN testing to increase the fault-detection capability of natural test input sets. Further, another study [17] found that retraining DNN models with new input sets that improve coverage does not help increase the robustness of

the model to adversarial attacks.

Furthermore, coverage criteria require full access to the internals of the DNN state or training data, both of which are often not available to testers especially when the DNN model is proprietary and provided by a third-party. Thus, in our project, we focus on black-box input diversity metrics in order to provide guidance on how to assess test suites or select test cases for DNNs. We target diversity since it has been successfully used in testing regular software systems [19], [20], [21]. Intuitively, relying on diverse test inputs should increase the exploration of the fault space and thus increase the fault detection capability of a given test input set. We therefore propose and investigate black-box diversity metrics for DNNs, investigate their relationships with coverage metrics, and analyse their association to fault detection. In other words, this paper focuses on the fundamental assumptions related to the relationship between testing criteria (i.e., coverage and diversity metrics) and faults in DNNs. However, we do not investigate in this paper how these testing criteria might be used for specific testing scenarios such as the selection, minimization, or generation of test sets. Nonetheless, investigating the relationship between DNN faults and testing criteria is an essential step for selecting proper testing criteria, independent of any specific purpose.

In traditional software systems, some of the inputs causing failures are usually very close to each other [22], [23]. Similarly, it has been observed that many mispredicted inputs in DNNs fail due to the same causes [24]. Counting such inputs for assessing the fault detection capability of a test suite is therefore misleading. However, the notion of fault, though rather straightforward in regular software, is elusive in DNNs. For this reason, we rely in this paper on a clustering-based fault estimation approach to group similar mispredicted inputs based on their features and misprediction behaviour [24]. We assume that each cluster corresponds to a fault as similar mispredicted inputs belonging to a same cluster are assumed to be mispredicted for similar reasons.

To assess test suites for DNNs, we consider and adapt three diversity metrics. As we consider in this paper datasets composed of images, commonly used as inputs in many DNNs (e.g., perception layer of cyber-physical systems), we rely on a feature extraction model to extract features from images that will be used to compute the diversity of test input sets. We evaluate the selected metrics in terms of their capability to measure actual diversity based on extracted features. We then analyse their associations with fault detection in DNNs using four widely-used datasets and five different DNN models. We further study state-of-the-art white-box coverage metrics and their associations with diversity and fault detection.

Based on our experiments, we show that diversity metrics, in particular Geometric Diversity (GD) [25], though black-box and not using any DNN internal information, far outperforms existing coverage criteria in terms of fault-revealing capability and computational time. We also show that state-of-the-art coverage metrics are not correlated to faults or diversity in natural test input sets.

Overall, the main contributions of our paper are as follows:

- We propose and study the usage of black-box diversity metrics to guide the test of DNN models. We show that geometric diversity is the best option in guiding the testing of DNN models since it is positively correlated to faults in subsets.
- We introduce and validate a clustering-based approach to estimate faults in DNNs as test input sets typically contain many similar mispredicted inputs caused by the same problems in the DNN model. We explain why this is a requirement to evaluate any test set evaluation criterion.
- We study state-of-the-art coverage criteria and show that there is no correlation between coverage and faults in DNN models. Further, coverage is also not correlated with diversity in input sets. Our results question the reliability of coverage, as currently defined, to guide the testing of DNNs if the objective is to detect as many faults as possible.

The remainder of the paper is structured as follows. Section 2 presents our approach and describes the selected diversity metrics. Section 3 presents our empirical evaluation and results. Section 4 discusses the implications of our results as well and our recommendations for guiding the testing of DNN models. Section 5 describes the threats to validity of our study. Sections 6 and 7 contrast our work with related work and conclude the paper, respectively.

2 APPROACH

A central problem in software testing, especially when test oracles (verdicts) are not automated, is the selection of a small set of test cases that sufficiently exercise a software system. Intuitively, testers should select a set of diverse test cases since selecting similar test cases does not bring extra benefits in terms of fault detection. In this paper, we aim to support testing of DNN models by studying diversity metrics to guide the selection, minimisation and generation of test inputs, relying on the best diversity metric in terms of both the capacity to uncover erroneous behaviour and computational complexity. To do so, we consider and adapt three diversity metrics that are a priori relevant and have been used in other contexts. We rely on a feature extraction model to extract features from images that we can rely on to compute diversity. In section 3, we will first evaluate the selected metrics in terms of their capability to measure the actual diversity of a test input set. We will then study their relationships with state-of-the-art white-box coverage metrics and analyse their associations with fault detection in DNNs.

In this section, we describe the feature extraction method and the diversity metrics that we considered and detail the evaluation process in the following section.

2.1 Feature Extraction

In order for diversity to account for the content of images, we need to extract features from each input image in the test input set. Consequently, we rely on VGG-16 [26], which is one of the most used and accurate state-of-the-art feature extraction models [27], [28]. It is a pre-trained convolutional neural network model and consists of 16 weight layers, including thirteen convolutional layers with filter size of 3x3, and three fully-connected layers. The model is

trained on ImageNet¹, which is a dataset of over 14 million labelled images belonging to 22000 categories.

We use VGG-16 to extract the features of images. A feature is an activation value on the layer after the last convolutional layer of the VGG-16 model. A set of features can characterize semantic elements such as shapes and colors. We extract the features in the test input set S and build the related feature matrix Vs where (1) each row of the matrix corresponds to the feature vector of an input in the test set, and (2) each column corresponds to a feature.

After generating the feature matrix we normalise it by applying *Min-Max normalization* per feature, which is one of the most common and simplest ways to normalise data. For each feature in Vs , the maximum and minimum values of that feature are transformed to one and zero, respectively, and every other value is transformed to a real value between zero and one. The *Min-Max normalization* is defined as follows. For every feature Vs_j in the feature matrix Vs where $j \in [1, 2, \dots, m]$ and m is the number of features, the normalized feature Vs'_j is calculated as follows:

$$Vs'_j(i) = \frac{Vs_j(i) - \min(Vs_j)}{\max(Vs_j) - \min(Vs_j)} \quad (1)$$

We normalise the feature matrix (1) to make the computation of the selected diversity metrics more scalable, and (2) to eliminate the dominance effect of features with large value ranges.

2.2 Diversity metrics

In this section, we describe the selected diversity metrics: Geometric Diversity [25], [29], Normalized Compression Distance [30], [21], and Standard Deviation. We have chosen these three metrics because they measure and quantify diversity in subsets. Furthermore, these metrics are widely used in the literature. For instance, the geometric diversity metric has been used in a variety of machine learning applications such as the selection of training sets with the Determinantal Point Process method [25], data summarization [31] and data clustering [32], [33]. Furthermore, the standard deviation metric is considered one of the state-of-the-art diversity metrics that has been successfully applied to measure text and image similarity [34]. Finally, the NCD metric has been also employed in many application domains such as image processing [30], security [35] and clustering [36], [30]. This metric supports any type of inputs and has been recently used to guide the selection of diverse input tests for regular software systems [21].

We will describe in this section each of these metrics and discuss their strengths and limitations.

2.2.1 Geometric Diversity

We consider the geometric diversity (GD) metric to measure the diversity of the selected inputs [25]. As mentioned earlier, this metric is widely used to select diverse input sets with the Determinantal Point Process (DPP) method [25], [29]. In fact, DPP is applied to guide the selection of diverse subsets from a fixed ground set [37] and has been used in a variety of machine learning applications for images [25], videos [38], documents [31], recommendation systems [39],

and sensor placement [40]. The key characteristic of DPP is that the inclusion of one item makes including other similar items less likely, i.e., a DPP assigns a greater probability to subsets of items that are diverse. Thus, a DPP value of a subset indicates its diversity where the higher this value, the more diverse the subset. The key component in DPP is geometric diversity that measures the diversity of an input set in terms of the (hyper)volume spanned by the input feature vectors (feature matrix).

2.2.1.1 Definition

The geometric diversity $G(\cdot)$ is defined as follows. Given a dataset X , a number of inputs n , a number of features m , and feature vectors $V \in R^{n \times m}$, the geometric diversity of a subset $S \subseteq X$ is defined as:

$$G(S) = \det(Vs * Vs^T) \quad (2)$$

which corresponds to the squared volume of the parallelepiped spanned by the rows of Vs , since they correspond to vectors in the feature space. The larger the volume, the more diverse is S in the feature space, as illustrated in Figure 1. Indeed, very different (similar) images are expected to result into very different (similar) feature vectors.

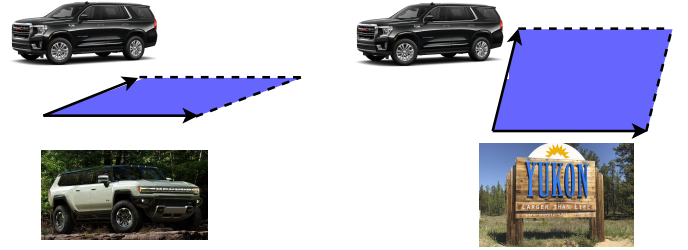


Figure 1: Illustration of the geometric diversity metric

2.2.1.2 Calculation

The geometric diversity takes as input the feature matrix of the test input set, as generated using the feature extraction model. Because geometric diversity relies on the calculation of the determinant of a matrix, we need to handle several challenges related to such processing:

Determinant Overflow. The determinant is likely to run into overflow when we deal with large features matrices. The main cause of the problem is that the determinant value is too large to be represented by a real number. To overcome this problem, we follow the recommendations of Celis *et al.* [41] and consider the logarithm of this value rather than the determinant itself. We also overcome the determinant overflow problem by considering the normalized feature matrix Vs' and thus make the computation of GD more scalable.

Mathematical Limitations. If a matrix contains at least two linearly dependent vectors, then its determinant will be equal to zero. Consequently, we cannot calculate the geometric diversity score of an input set that contains duplicate inputs. The feature extraction model predicts features for each test input. If the feature values are the same for two test inputs, then we have duplicate inputs. This means the two test images are redundant in terms of this feature extraction

1. <https://image-net.org/index.php>

model. We therefore have to delete redundant inputs before calculating the diversity score. This kind of pre-processing is acceptable in our context because (1) duplicate inputs do not bring any value for testing our model, and (2) we aim to test the DNN model with a diverse input set to detect faults.

Further, the maximum subset size for which we calculate GD must be less than the number of the features in V_s . This is also due to the mathematical limitations of the determinant and the rank of matrices.

Proof: In linear algebra, the rank of a matrix A of size $n * m$ refers to the number of linearly independent rows or columns in the matrix. Consequently $Rank(A_{n*m}) \leq \min(n, m)$, where n is the number of lines in the matrix A , and m is the number of columns. Let us consider a square matrix B of size $n * n$. By definition, If $Rank(B) < n$ then $Det(B) = 0$. Let us assume that $B = A * A^T$. By definition $Rank(B) = Rank(A * A^T) = Rank(A)$. If $n > m$ then $Rank(B) \leq m < n$. As a result $Det(B) = Det(A * A^T) = 0$.

To overcome this mathematical limitation of GD, we can select one of the internal layers of the feature extraction model to obtain more features and be able to compute GD for more inputs. We suggest to start with the last hidden layers of the feature extraction model since, as noted by Bengio et al. [42], [10], deeper layers represent higher level features of the input. In other words, the last hidden layers are likely to contain the most semantically meaningful and helpful features to characterise an input.

2.2.2 Normalized Compression Distance

The Normalized Compression Distance (NCD) is a similarity metric based on the Kolmogorov complexity [43] and information distance [44] where we measure the information required to transform one object into another to assess the similarity between these objects. Because of the complexity of calculating the Kolmogorov complexity, we approximate it through using real-world compressors [30], [45]. This leads to the normalized compression distance [36] which has been extended by Cohen *et al.* [30] to support the calculation of multisets' similarity.

2.2.2.1 Definition

The NCD metric for a multiset S is calculated via an intermediate measure NCD_1 [30], [46], [21]:

$$NCD_1(S) = \frac{C(S) - \min_{s \in S} \{C(s)\}}{\max_{s \in S} \{C(S) \setminus \{s\}\}} \quad (3)$$

$$NCD(S) = \max \left\{ NCD_1(S), \max_{Y \subset S} \{NCD(Y)\} \right\} \quad (4)$$

where $C(S)$ denotes the length of S after compression. NCD supports any type of inputs (e.g, text, images, execution traces, etc.) and has found many applications in pattern recognition [47], [48], clustering [30], [36], security [35] and measuring the diversity of test sets [21], [49].

2.2.2.2 Calculation

We have re-implemented the NCD metric for multisets based on the original paper. NCD takes as input the normalized feature matrix of an input set and measures its diversity score. NCD takes values in the range $[0, 1]$. The more diverse the input set, the larger the NCD score. However, one of the limitations of such metric is its high computational

cost, such that its application on large input sets becomes prohibitive [30], [21]. Also, NCD is highly sensitive to the used compression tool [21]. Different compression tools determine various performance aspects of NCD, such as computation time, used memory, and compression distance. Following the recommendations of existing NCD-related papers [21], [30], [35], we have tried different compression tools like *Lzm*, *Bzip2*, and *Zlip*. We tested their efficiency in terms of computational cost and correctness in generating the diversity scores. We evaluated the correctness of the diversity scores by controlling the actual diversity of input sets in terms of features and comparing the corresponding NCD scores. More precisely, we compared the NCD score of input sets having similar images with other sets having different images. The NCD score is expected to increase when the input set is more diverse in terms of features. Finally, the best results were obtained with *Bzip2* which was used in our experiments.

2.2.3 Standard Deviation

Standard deviation (STD) is a statistical measure of how far from the mean a group of data points is, by calculating the square root of the variance.

2.2.3.1 Definition

STD is a quite straightforward measure of the diversity of a test input set based on the statistical variation of the inputs' features. We define the STD metric as the norm of the standard deviation of each feature in the test input set. More formally, we define STD of an input set S of size n as follows:

$$STD(S) = \left\| \left(\sqrt{\sum_{i=1}^n \frac{Vs_{i,j} - \mu_j}{n}}, j \in [1, m] \right) \right\| \quad (5)$$

where V_s is the feature matrix of the input set S , m is the number of features, and μ_j is the mean value of feature j in V_s .

2.2.3.2 Calculation

To calculate STD for an input set S , we should first extract the feature matrix for S and normalise it. We then calculate the norm of the standard deviations of each feature in the matrix to measure the diversity of the input set. The higher STD, the more diverse the input set. One of the limitations of the standard deviation is its dependence to the mean, which introduce unwanted bias in some cases. To explain this issue, let us consider two subsets A and B of the same size where (1) in subset A we have two sets of similar inputs and these two sets are very far from each other in the features space, and (2) in subset B all inputs are very different from each other. The variance of the inputs in subset A with respect to the mean could be larger than the one in subset B . In such a case, $STD(A)$ would be larger than $STD(B)$ though subset B is more diverse than A , as the latter only contains two truly distinct groups of inputs.

3 EMPIRICAL EVALUATION

This section describes the empirical evaluation of our approach, including research questions, datasets, DNN models, experiments and results.

Dataset	Description	DNN Model	Accuracy
MNIST	Handwritten digit images composed of 60,000 images for training and 10,000 images for testing.	LeNet-5	87.85%
		LeNet-1	84.5%
Fashion-MNIST	Grayscale images in 10 different classes of clothes composed of 60,000 images for training and 10,000 images for testing.	LeNet-4	88%
Cifar-10	Object recognition dataset in ten different classes composed of 50,000 images for training and 10,000 images for testing.	A 12-layer ConvNet with max-pooling and dropout layers.	82.93%
		ResNet20	86%
SVHN	A real-world image dataset for recognizing house numbers obtained from Google Street View images. It is composed of 73,257 training images and 26,032 testing images.	LeNet-5	88%

Table 1: Datasets and models used for evaluation

3.1 Research Questions

Our empirical evaluation is designed to answer the following research questions.

- **RQ1. To what extent are the selected diversity metrics measuring actual diversity in input sets?** We want to assess, in a controlled way, the reliability of the selected diversity metrics for measuring the actual diversity of an input set in terms of the features the images contain. Only the metrics that will reliably reflect changes in image diversity will be retained for the next research questions.
- **RQ2. How does diversity relate to fault detection?** Similar to other studies in different contexts [21], [50], [51], we want to investigate the correlation between diversity and faults to assess whether diverse input sets lead to higher fault coverage. We do not investigate in this research question the correlation between diversity and the number of mispredicted inputs as this is misleading. Indeed, similar to failures in regular software, many mispredictions result from the same problems in the DNN model and are therefore redundant. In classification problems, for example, guiding the selection of test inputs to maximise misprediction rates (the number of mispredicted inputs / total number of inputs) could thus be misleading. However, the notion of fault in DNN models is not as straightforward as in regular software, where you can identify statements responsible for failures. Therefore, to investigate this research question, we need to first define a mechanism to compare how effective test sets are at detecting faults in DNNs, so that we can then investigate the relationship between diversity and faults.
- **RQ3. How does coverage relate to fault detection?** Similar to diversity, we want to assess the association between state-of-the-art coverage metrics and faults. This will enable us to compare black-box diversity and white-box coverage in terms of the guidance they can provide to select test sets with high fault revealing power. Note that recent studies questioned the use of coverage metrics to assess DNN test inputs [16], [52]. In fact, state-of-the-art coverage metrics highly rely on artificial inputs generated based on adversarial methods [12], [13], [14], [10], [11]. However, their positive correlation with the presence of adversarial inputs does not necessarily mean that they are efficient to reveal the fault detection capability of natural test input sets. Several studies [16], [18] have actually failed to find strong correlation between coverage and misprediction rates when using only natural input sets. Furthermore, coverage metrics showed poor performance in guiding the retraining of DNN models to improve the robustness of the model to adversarial attacks [17], [53]. Therefore, there is still no consensus on which coverage metrics are suitable for different DNN testing-related tasks such as test selection, minimisation, and generation.
- **RQ4. How do diversity and coverage perform in terms of computation time?** We want to compare the selected diversity and coverage metrics in terms of their computation time. Most importantly, we aim to study how such computation times scale as the size of test sets increases. Excessive computation times may limit applicability, though what is acceptable depends on context.
- **RQ5. How does diversity relate to coverage?** Though diversity is black-box and has therefore inherent practi-

cal advantages, it is interesting to study the correlation between diversity and coverage to determine if they essentially capture the same thing. Though this question can be indirectly answered with some of the previous questions, such correlation analysis can provide additional insights to explain and support previous results.

3.2 Subject Datasets and DL Models

Table 1 shows the characteristics of the datasets and models in our experiments. We consider four widely used image recognition datasets which are Cifar-10 [54], MNIST [55], Fashion-MNIST [55] and SVHN [56]. We use these datasets with five state-of-the-art DNN models: 12 layers Convolutional Neural Network (12-layer ConvNet), LeNet-1, LeNet-4, LeNet-5, and ResNet20.

Cifar-10 contains 50,000 images for training and 10,000 for testing. All these images belong to 10 different classes (e.g. cats, dogs, trucks). We also consider MNIST, which contains 70,000 images (60,000 for training and 10,000 for testing). Each of these images represents a handwritten digit and belongs to one of 10 classes. We include as well Fashion-MNIST, which contains grayscale images in 10 different classes of clothes. It is composed of 60,000 images for training and 10,000 images for testing. Finally, we consider SVHN, a real-world image dataset for recognizing house numbers. It contains 99,289 images where 73,257 images are for training and 26,032 images are for testing. For Cifar-10, we use a 12-layer ConvNet and ResNet20 that we train for 50 and 100 epochs, respectively. For MNIST, we use the LeNet-1 and LeNet-5 models that we train for 50 epochs. We train the LeNet-4 model with Fashion-MNIST for 20 epochs. Finally, for SVHN, we use the LeNet-5 model that we train for 100 epochs. The different combinations of models and datasets, along with the models’ accuracy, are detailed in Table 1.

We selected these datasets and models because they are widely used in the literature [12], [10], [11], [13]. Further, all the inputs in the selected datasets are correctly labelled. Finally, these datasets and models are considered good baselines to observe key trends as they offer a wide range of diverse inputs (in terms of classes and domain concepts) and different models (in terms of internal architecture).

3.3 Evaluation and Results

Before addressing our research questions, one essential issue is how to count faults in DNNs. A misprediction implies the existence of a fault in the DNN. However, identifying faults is not as straightforward as in regular software where faulty statements causing failures can be identified. Nevertheless, estimating fault detection effectiveness is essential to be able to compare coverage and diversity metrics. Indeed, simply comparing misprediction rates is misleading as many test inputs are typically mispredicted for the same reasons [24]. Typically, with regular software, a tester does not seek to select input tests aiming at maximising the failure rate (equivalent to the misprediction rate in our context) but rather wants to maximise the number of distinct detected faults. This should be not different with DNNs where we want to detect distinct causes for mispredictions.

We illustrate this issue in Figure 2 where we represent an example of a test input set in a two-dimensional feature

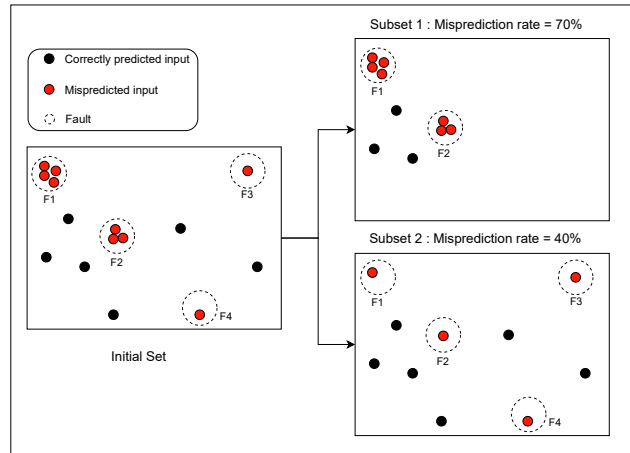


Figure 2: Relying on misprediction rates is misleading

space. Black dots refer to the inputs correctly predicted by the DNN under test while red dots represent the mispredicted ones. We select two subsets from the initial set and measure their corresponding misprediction rates. As we can see in Figure 2, subset 1 is less diverse than subset 2 but has a higher misprediction rate. However, some of its mispredicted inputs are very similar and somewhat redundant. As a result, it can be argued that subset 2 is more diverse than subset 1 and is more informative for testing the model since its mispredicted inputs can potentially reveal more faults in the DNN model. Also, when considering in preliminary experiments (not included in this paper) the computation of misprediction rates in test input sets and studying their correlation with diversity and coverage, we found no statistically significant correlation for both diversity and coverage metrics. We suspected that accounting for a large number of redundant test inputs affected our correlation analysis. In any case, in practice, selecting or generating test inputs that trigger failures (i.e. mispredictions) is far more useful when these failures are diverse [57]. A test set that repeatedly exposes the same problem in the DNN model is a waste of computational resources, especially when we have a limited testing budget and a high labeling cost for testing data [57]. This is why, similar to other studies comparing the effectiveness of test strategies with regular software, we want here to address the notion of faults detected in DNNs and study their association to diversity and coverage.

3.3.1 Estimating Faults in DNNs

Following a similar approach to the work of Fahmy *et al.* [24] and Attaoui *et al.* [58], we rely on a clustering approach to group similar mispredicted inputs presenting a common set of characteristics that are plausible causes for mispredictions. We approximate the number of detected faults in a DNN through such clustering. Indeed, though many mispredicted test inputs are redundant and due to the same causes, we assume that test inputs belonging to different clusters are mispredicted due to distinct problems [24] in the DNN model. This is of course an approximation but a practical and plausible way to estimate and compare the number of detected faults across coverage and diversity strategies. Though faults can only be addressed

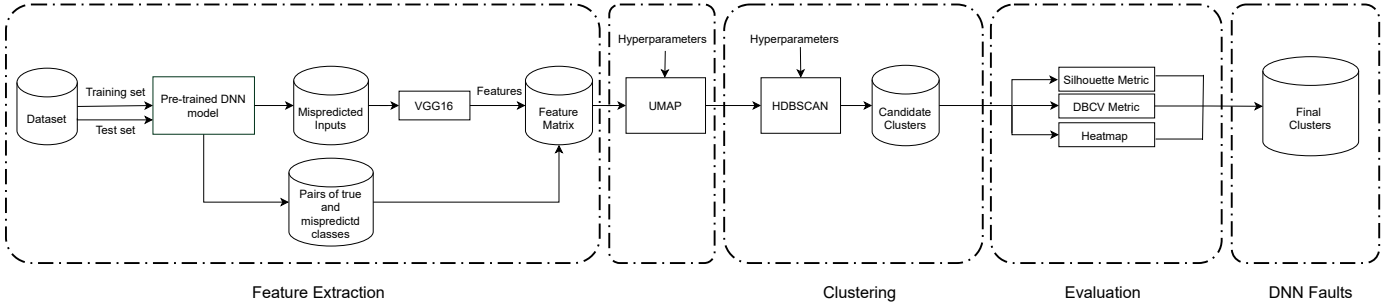


Figure 3: Estimating faults in DNNs

by re-training in DNNs, as opposed to debugging, clusters nevertheless capture common causes for mispredictions and are thus comparable to faults in regular software. Figure 3 depicts the approach for counting faults in DNNs and we describe each of its steps in detail below.

3.3.1.1 Feature Extraction

We start by training our model using the training dataset. We then run our pre-trained model on the test and training datasets to identify all mispredicted inputs. We not only consider mispredicted inputs from the test set, but also use mispredicted inputs from the training dataset to extract the best clusters possible and therefore estimate detected faults as accurately as we can in our experiments. We rely on VGG16 to extract the features of the mispredicted inputs and build the corresponding feature matrix as described earlier in section 2.1. We add two extra features to the matrix from the DNN model to capture actual and mispredicted classes related to each misclassified input. This is meant to add information to the feature matrix about the misprediction behaviour of the model under-test for each mispredicted input, which we believe can help build better clusters to reflect common misprediction causes.

3.3.1.2 Dimensionality Reduction

By definition, the number of input features for a dataset corresponds to its dimensionality. Low density in high dimensional spaces makes it difficult in general, for typical clustering algorithms, to find a continuous boundary that separates the different clusters [59]. Therefore, employing dimensionality reduction techniques can help clustering algorithms make the inputs and their related clusters more distinguishable. Because we are dealing with high dimensional inputs (512 features from VGG model and two features from the DNN model), we rely on the Uniform Manifold Approximation and Projection (UMAP) [60] dimensionality reduction technique. We selected UMAP because several studies [61], [62] have shown its effectiveness as a pre-processing step to boost the performance of clustering algorithms when compared to other state-of-the-art dimensionality reduction techniques such as PCA [63] and t-SNE [64]. In fact, PCA is a linear dimensionality reduction technique that performs poorly on features with nonlinear relationships. Therefore, in order to deal with high-dimensionality data to obtain low-dimensionality and nonlinear manifolds, some nonlinear dimensionality reduction algorithms such as UMAP and t-SNE should be used [62]. However, t-SNE is more computationally expensive than UMAP and PCA. It

is used in practice for data visualisation and data reduction to two or three dimensions. Furthermore, it involves hyperparameters that are not always easy to tune in order to get the best results. Therefore, we relied for our study on UMAP for dimensionality reduction, as an effective pre-processing step to boost the performance of density-based clustering that will be used in the next step.

3.3.1.3 Clustering

After performing dimensionality reduction, we apply the HDBSCAN [65] clustering algorithm to group mispredicted inputs that are similar and believed to be due to the same causes (faults) in the DNN model. HDBSCAN is a density-based clustering algorithm where each dense region is considered a cluster and low-density regions are considered noise. In other words, it views clusters as areas of high density separated by areas of low density. Clusters found by HDBSCAN can be of any shape, as opposed to other types of clustering algorithms, such as k-means or hierarchical clustering, which assume that clusters are convex shaped. Each cluster is supposed to correspond to a fault (common problems) in the DNN model as its inputs are similar in terms of extracted features as well as actual and mispredicted classes.

3.3.1.4 Evaluation

Like for any clustering algorithm, there are several hyperparameters to fine tune in order to obtain the best clustering results. Such hyperparameters include, for example, the minimum distance that controls how tightly UMAP is allowed to pack points together, the number of neighbours to consider as locally connected in UMAP, and the minimum size of clusters in HDBSCAN. We tried several hyperparameter configurations and selected the best configurations based on both manual and metric-based evaluations. For the latter, more specifically, we relied on two standard metrics to evaluate the clusters, which are the Silhouette score [66] and the Density-Based Clustering Validation (DBCV) [67] metric.

The Silhouette score is one of the state-of-the-art clustering evaluation metrics that compare inter- and intra-cluster distances. It varies between -1 and 1. The closer to 1, the better the clustering. A score near zero represents clusters with inputs very close to the decision boundary of the neighboring clusters. A negative score indicates that the inputs are generally assigned to the wrong clusters.

We also relied on the DBCV metric to evaluate the generated clusters. This metric is dedicated to density-

Dataset	Model	#Misp. in training set	#Misp. in test set	Silh.	DBCW	#Noisy test inputs	#Clusters
MNIST	LeNet-5	8055	1215	0.64	0.68	58	85
MNIST	LeNet-1	9754	1542	0.71	0.74	72	137
Fashion-MNIST	LeNet-4	5636	1157	0.65	0.53	101	141
Cifar-10	12-layer ConvNet	1173	1707	0.71	0.62	56	187
Cifar-10	ResNet20	2191	1384	0.75	0.63	78	177
SVHN	LeNet-5	151	3009	0.69	0.59	213	147

Table 2: Fault estimates across datasets and models

based clustering algorithms and assesses clustering quality based on the relative density connection between pairs of inputs. It evaluates the within- and between-cluster density connectedness [68]. Similar to Silhouette, DBCW generates scores between -1 and 1 [67]. High density within clusters and low density between clusters lead to high DBCW scores, indicating better clustering results.

We selected the configuration with the best Silhouette and DBCW scores. We further evaluated the generated clusters by performing a manual evaluation. We tried to check first the content of the clusters to see whether their inputs are similar or share at least some features that may lead to mispredictions by the DNN model. Because of the large number of mispredicted inputs, an exhaustive manual inspection of the clusters is unpractical. Therefore we relied on generating the features’ heatmaps related to each cluster to better visualise and assess the quality of the clusters. Figures 4, 5, 6 and 7 illustrate four representative examples of heatmaps where rows correspond to the inputs’ ids in one cluster, columns refer to their features, and colours encode the features’ values. As we observe in Figures 4, 6, and 7, within a cluster, well-clustered inputs share common patterns in terms of the features’ distribution while ill-clustered inputs (such as noisy inputs) do not, as visible in Figure 5. Based on our manual analysis of the final selected clusters, we observed that most of them look like the first three figures and share common patterns. We therefore conclude that the mispredicted inputs inside each cluster are similar and share common characteristics (features) potentially causing mispredictions.

Table 2 describes the final clusters that we generated for the different datasets and models that we considered in our experiments. We observe that the number of noisy inputs (inputs that do not belong to any cluster) is not large compared to the total number of mispredicted inputs. We decided to delete them from the sets of mispredicted inputs in all the following experiments (1) as they do not belong to any cluster and cannot therefore be associated with faults as we defined them, and (2) the minimum number of detected faults in the studied DNN models can thus be assumed to correspond to the number of clusters.

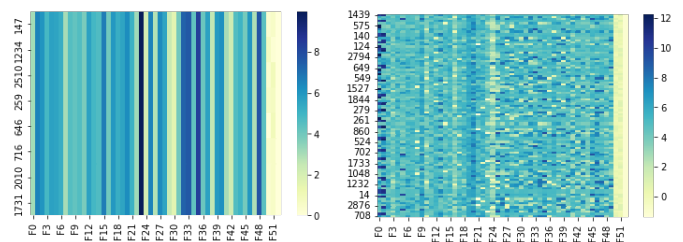


Figure 4: Heatmap example 1 related to a final cluster

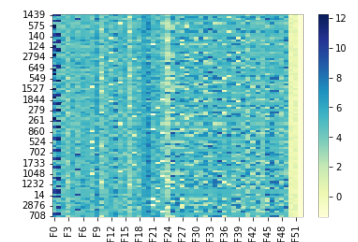


Figure 5: Heatmap example 2 related to noisy cluster

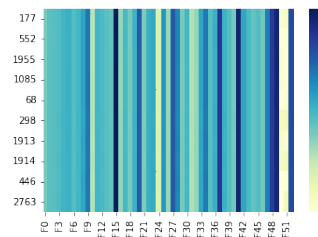


Figure 6: Heatmap example 3 related to a final cluster

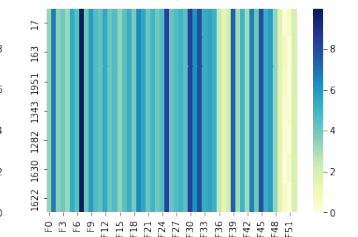


Figure 7: Heatmap example 4 related to a final cluster

3.3.1.5 Validation

As mentioned earlier, we followed an approach similar to existing work [24], [58] to estimate faults in DNNs. The authors conducted an empirical study on six DNNs to validate the clustering-based fault estimation approach. They retrained the DNNs using the original training set and subsets selected from each identified cluster (i.e., fault), which led to a significant improvement of the models’ accuracy, thus demonstrating the usefulness of clustering. To further validate the identified faults (clusters) in our work, we follow a finer-grained validation method which aims at proving that (1) inputs in the same cluster tend to be mispredicted due to the same fault, and (2) inputs belonging to different clusters are mispredicted because of distinct faults.

Inputs that belong to the same cluster are mispredicted due to the same fault in the DNN model. If inputs within one cluster are mispredicted due to the same fault, retraining the model with a subset of the cluster should help fix the

Model	Faults C_i	Accuracy on the retraining cluster C_i	Average Accuracy on the other clusters $C_{j \neq i}$
12-layer ConvNet	Cluster 1	80%	28.23%
	Cluster 2	60%	27.42%
	Cluster 3	55%	27.45%
	Cluster 4	71.40%	27.06%
	Cluster 5	66.70%	27.40%
	Cluster 6	60%	27.95%
	Cluster 7	58.33%	27.76%
	Cluster 8	67.70%	28.60%
	Cluster 9	66.30%	27.74%
	Cluster 10	61%	27.80%
Average		66.64%	27.74%
ResNet20	Cluster 1	77%	30%
	Cluster 2	75%	29%
	Cluster 3	74%	28%
	Cluster 4	62.5%	31%
	Cluster 5	65%	29%
	Cluster 6	56.5%	28.70%
	Cluster 7	78.40%	30.3%
	Cluster 8	75%	29.9%
	Cluster 9	62.5%	31%
	Cluster 10	64%	31%
Average		69%	29.80%

Table 3: The results of faults validation experiment on 12-layer ConvNet and ResNet20. In each row, we retrained the model under test on 85% of each cluster C_i . We report in the third column the accuracy of the retrained model on the remaining 15% of cluster C_i . The last column refers to the average of accuracies of the retrained models over all other fault clusters C_j ($j \neq i$)

model with respect to that fault. We verify such hypothesis for each fault-related cluster C_i where $i \in [1, 2, \dots, n]$ and n is the total number of the identified faults (clusters), by retraining the original DNN model under test with a retraining dataset consisting of the union of the original training set and 85% of randomly selected mispredicted inputs inside C_i . The original training set is reused to prevent any reduction in model accuracy [24], [58], [69]. We then test the retrained model on the remaining 15% of inputs in C_i . We repeat this process five times (as we randomly select inputs from cluster C_i) and measure the average accuracy of the retrained models when tested with 15% of the remaining inputs from cluster C_i . If clusters indeed include mispredictions caused by the same fault, the retraining process is expected to alleviate the cause for input mispredictions in C_i and thus significantly improve the accuracy of the model for images in that particular cluster. We do not expect a perfect model with no mispredictions since we do not have large number of mispredicted inputs in each cluster to retrain the model. Moreover, clustering is not expected to be perfect but only an approximation of faults. Since clusters do not have the same size and are not all large enough to enable the above analysis, our analysis focuses on the ten largest clusters across datasets and models. Due to the high computational expense of our experiments, we considered two models which are 12-layer ConvNet and ResNet20 to validate the used fault estimation method. Thus, we report in Table 3 the accuracy of the retrained 12-layer ConvNet models and ResNet20 when tested on the ten largest clusters

in each of their corresponding dataset. Let us recall that, by definition, the accuracy of the original model on all cluster images was zero since they were all mispredicted. As shown in Table 3, we get significant improvements in terms of models' accuracy with an average equal to 66.64% in 12-layer ConvNet and 69% in ResNet20. Results therefore suggest that test inputs belonging to the same cluster are indeed mispredicted due to the same faults, thus supporting the hypothesis underlying our method to count faults.

Inputs belonging to different clusters are mispredicted due to distinct faults. If the clusters represent distinct faults in the DNN, retraining the model with a subset of a cluster C_i should have a much more significant effect on the other images in C_i when compared to images in other clusters. Consequently, to validate that inputs belonging to different clusters are mispredicted due to distinct faults, we test each of the previously retrained DNN models for each cluster C_i , on the other clusters C_j where $j \neq i$. We measure the average accuracy of each of the retrained DNN models over all remaining clusters and report the results in Table 3. As we can see, the retrained ResNet20 and 12-layer ConvNet models are significantly more accurate on the clusters for which they were retrained than on other clusters. Indeed, in 12-layer ConvNet for example, the average accuracy for the latter is only 27.74% compared to 66.64% for the former. We therefore conclude that inputs belonging to different clusters tend to be mispredicted due to distinct faults. Note that, though they are much more limited, we nevertheless observed improvements in model accuracy on clusters for

which the model was not retrained. This can be expected since fixing one fault in the DNN model through retraining may also, to a more limited extent, fix other related faults, thus potentially improving the accuracy on other clusters as well. Finally, as acknowledged earlier, our clustering is not perfect and although the silhouette and DBCV scores of the obtained clusters are high, they are not equal to one as we can see in Table 2.

3.3.2 RQ1. To what extent are the selected diversity metrics measuring actual diversity in input sets?

To directly evaluate the capability of the selected metrics to actually measure diversity in input sets, we study how diversity scores change while varying, in a controlled manner, the number of image classes covered by the input sets. Classes characterise the content of images. For example, a set of images, sampled from the Cifar-10 dataset, containing the two classes *Car* and *Deer* is considered more diverse than a set containing only *cars*. We assume that diversity scores should increase with the number of classes that are present in an input set.

Algorithm 1 describes at a logical level our experiment procedure to answer RQ1. This procedure aims at increasing actual diversity of the content of image sets in a controlled manner and observe whether diversity metrics are sensitive to such changes. Given a certain dataset, we start by randomly selecting the first class C_i from the dataset in our experiment (Line 1). Then, we randomly sample, with replacement, 20 input sets of size 100. Each of these input sets are sampled from the same class C_i (Lines 2-4). We measure the diversity scores for each initial input set (Lines 5-7). For each such input set, we incrementally increase the number of classes it covers by replacing some of its inputs with new ones from a new class $C_{k \neq i}$ while maintaining a uniform distribution across classes inside the samples. To do so, for each initial input set $Fset$, we randomly select another class C_k that we want to add (Lines 8 and 10) and randomly select new inputs from the class C_k as a *Newset* (Line 10-11). We randomly keep about $100/k$ inputs (k is the number of selected classes) of each existing class in $Fset$ (Line 12) and merge their inputs in $Fset$ with the newly selected ones in *Newset* (Line 13). Finally, we measure the diversity scores for each input set (Lines 15-17) and repeat the process until we include images from all classes in the selected dataset (Line 9). We report the distribution of the diversity scores that are related to each metric using boxplots, as depicted in Figure 8. Each boxplot illustrates the distribution of the diversity scores of 20 input sets of size 100, each having the same number of classes.

For example, when we consider Cifar-10, we start by selecting 20 input sets of size 100. All the selected images inside each input set correspond to the class *deer*. For each selected input set, we measure the GD, NCD and STD scores. For each metric, we report the distribution of the diversity scores related to these samples using boxplots, as depicted in Figures 8.a, 8.b and 8.c. We then increase the number of classes inside each sample by randomly replacing 50 images in *Deer* with new images from the *Truck* class. Each input set contains equal distribution of images of *Deer* and *Truck*. We report again the distribution of the diversity scores using boxplots. We repeat the process until we reach

Algorithm 1: Experimental Procedure for RQ1

```

Input:  $C$ : set of  $n$  classes in the dataset
          ( $C \leftarrow \{c_1, c_2, \dots, c_n\}$ )
Output:  $GDs, STDs, NCDs$ 
1  $c_i \leftarrow RandomClassSelect(1, C)$ 
2 for  $j$  in  $\{1, 2, \dots, 20\}$  do
3    $k \leftarrow 1$ 
4    $Fset \leftarrow RandomInputSelect(100, c_i)$ 
5    $GDs \leftarrow GD(Fset)$ 
6    $STDs \leftarrow STD(Fset)$ 
7    $NCDs \leftarrow NCD(Fset)$ 
8    $C \leftarrow C \setminus \{c_i\}$ 
9   for  $k$  in  $\{2, \dots, c_n\}$  do
10     $c_k \leftarrow RandomClassSelect(1, C)$ 
11     $NewSet \leftarrow RandomInputSelect(100/k, C_k)$ 
12     $Fset \leftarrow Keep(100/k, Fset)$ 
13     $Fset \leftarrow Merge(Fset, Newset)$ 
14     $C \leftarrow C \setminus \{c_k\}$ 
15     $GDs \leftarrow GD(Fset)$ 
16     $STDs \leftarrow STD(Fset)$ 
17     $NCDs \leftarrow NCD(Fset)$ 
18 return  $GDs, STDs, NCDs$ 

```

a total number of 10 classes inside the selected samples, while maintaining at each sampling iteration a uniform distribution across classes inside the input sets.

Based on Figure 8, we observe that GD outperforms NCD and STD as it exhibits a monotonic increase when increasing the number of classes inside the input sets. As we see in Figures 8.a and 8.d, the more diverse the input sets are, the higher GD becomes in all datasets and models that we have considered. We observe a similar but more noisy trend for STD. If we take the example of STD scores for MNIST (Cf. Figure 8.e), we observe that these scores slightly decrease for samples embedding seven classes. A similar observation can be made with Cifar-10 when going from nine to ten classes (Cf. Figure 8.b).

Surprisingly, we found that NCD scores do not increase when input sets become more diverse. We also observe that this diversity metric has low variability in terms of the generated scores. In fact, as we can see in Figures 8.c and 8.f, the range of the calculated mean NCD scores for the different input sets in the experiment is between 0.9895 and 0.9913. We should note that we have tried, in our experiments with NCD, other types of features to further assess the reliability of this metric in evaluating diversity in our context. For this purpose, we have followed the recommendations of Cohen *et al.* [30] and calculated the NCD scores of the input sets based on the raw images from MNIST. However, we obtained similarly poor results as the NCD score did not consistently increase when input sets became more diverse. Besides its poor performance in measuring data diversity, we should note that NCD is computationally expensive. It took about one hour to calculate the NCD score for one input set of size 100, thus suggesting another limitation regarding its applicability in guiding the test of DNN models. We conclude that, in our context, this metric is neither practical nor reliable in measuring data diversity and is therefore excluded from the rest of our study.

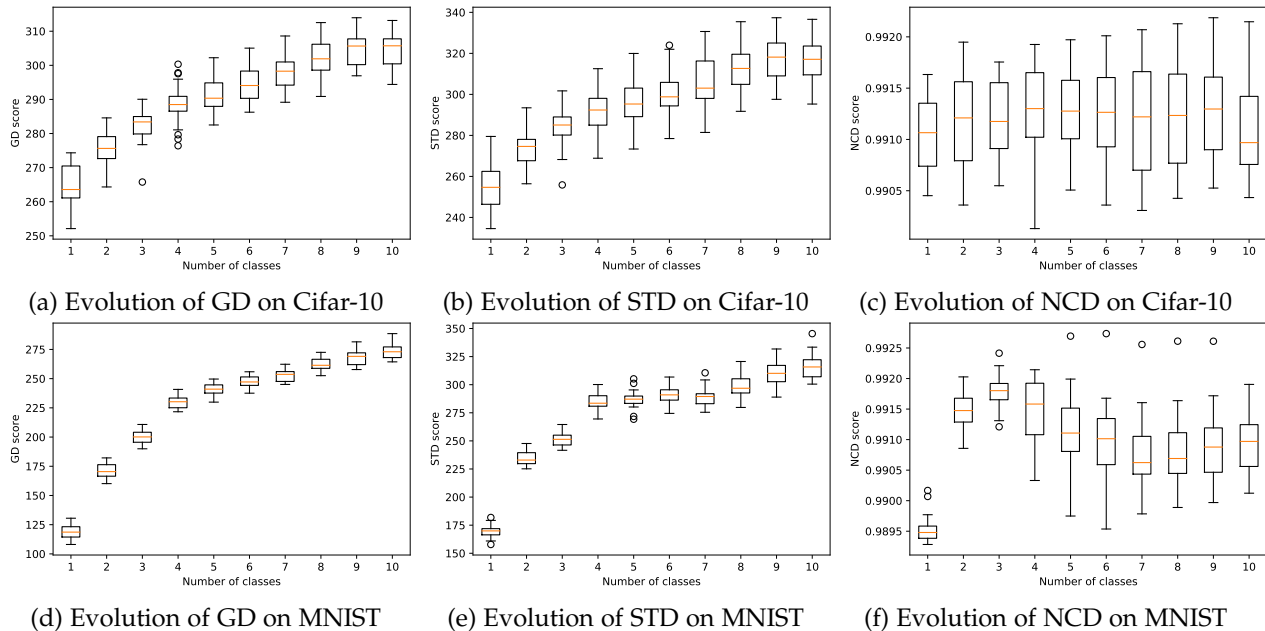


Figure 8: Evolution of the diversity scores for input sets from Cifar-10 and MNIST. Each boxplot shows the distribution of diversity scores of 20 input sets of size 100.

Answer to RQ1: GD and STD showed good performance in measuring actual data diversity in all the studied datasets. This is not the case of NCD, which we exclude from the following experiments.

3.3.3 RQ2. How does diversity relate to fault detection?

Dataset	Model	Test Set Size	Spearman	P-value
Cifar-10	12-layer ConvNet	100	8%	0.53
		200	17%	0.20
		300	-4%	0.78
		400	-9%	0.50
MNIST	LeNet-5	100	-27%	0.04
		200	4%	0.75
		300	-0.2%	0.98
		400	-10%	0.46

Table 4: Correlation between faults in subsets and clusters in the entire test set

We aim to investigate whether higher diversity increases the fault detection capability of test sets. For this purpose, we randomly select, with replacement, 60 samples of size $n \in \{100, 200, 300, 400, 1000\}$. For each sample, we calculate the corresponding diversity scores (GD and STD) and the number of faults. Finally, we calculate the Spearman correlation [70] between diversity scores and the number of faults, and report the correlation results in Tables 5, 6, 7, and 8, for the different datasets and DNN models. The grey boxes in the table refer to statistically significant correlations (p -value ≤ 0.05). We choose to use the Spearman correlation since it measures the strength of a monotonic correlation between two variables, without making assumptions about the form of the relationship or data distributions [70].

Nonetheless, there is a potential confounding factor for the correlation between faults and diversity. In the test dataset, if we were to apply clustering, we would expect higher diversity to lead to more clusters. If there is high similarity in distribution between the entire test dataset and the subset of mispredicted inputs, the correlation between diversity and faults in subsets could be due to the presence of such confounding factor. To check whether this is indeed a reality, we analyzed the correlation between the number of clusters in the entire test dataset that are covered and the number of faults (i.e, fault-related clusters) in subsets. A low correlation would then indicate that such a threat is unlikely.

We therefore applied the same HDBSCAN clustering process (section 3.3.1) to the entire testing dataset to obtain data clusters. We then considered the previously selected 60 samples of size $n \in \{100, 200, 300, 400\}$ and calculated the number of faults and data clusters inside each sample. Finally, we calculated the Spearman correlation between the number of faults and the number of covered data clusters in subsets. We performed this experiment using 12-layer ConvNet (with Cifar-10) and LeNet-5 (with MNIST) and report the correlation results in Table 4. As shown in the table, we did not find any positive and statistically significant correlation between faults and data clusters. We therefore conclude that there is no confounding factor in our correlation study between diversity and faults, thus giving us more confidence about the cause-effect relationship underlying the observed correlation between test suite diversity and faults, as described in the following.

In our correlation experiment between diversity and faults, we have considered a total of 60 configurations related to diversity metrics (6 models & datasets \times 2 diversity metrics \times 5 input sizes). We found that GD outperforms STD in terms of fault-revealing capabilities as we observe that there is a positive statistically significant correlation

Dataset	Model	Metric	Test Set Size	Spearman	P-value		
Cifar-10	12-layer ConvNet	GD	100	29%	0.02		
			200	32%	0.01		
			300	25%	0.05		
			400	31%	0.02		
			1000	29%	0.02		
		STD	100	26%	0.05		
			200	26%	0.05		
			300	19%	0.14		
			400	21%	0.11		
			1000	33%	0.01		
		LSC	100	8%	0.53		
			200	4%	0.74		
			300	0.5%	0.97		
			400	5%	0.70		
			1000	-5%	0.70		
		DSC	100	2%	0.85		
			200	18%	0.18		
			300	3%	0.80		
			400	-8%	0.55		
			1000	24%	0.07		
		NC	100	-22%	0.10		
			200	5.3%	0.69		
			300	0.3%	0.98		
			400	22%	0.10		
			1000	14%	0.28		
		KMNC	100	0.51%	0.97		
			200	14%	0.29		
			300	12%	0.35		
			400	-4%	0.76		
			1000	19%	0.15		
		NBC	100	15%	0.27		
			200	5.6%	0.67		
			300	7%	0.58		
			400	-0.6%	0.96		
			1000	11%	0.40		
		TKNC	100	15%	0.27		
			200	36%	0.005		
			300	28%	0.031		
			400	27%	0.04		
			1000	0.2%	0.98		
		SNAC	100	16%	0.22		
			200	5%	0.70		
			300	8%	0.52		
			400	-2%	0.89		
			1000	15%	0.24		
		MNIST	LeNet-5	GD	100	34%	0.009
					200	26%	0.04
					300	33%	0.01
400	37%				0.004		
1000	35%				0.005		
STD	100			6%	0.67		
	200			26%	0.04		
	300			34%	0.01		
	400			23%	0.07		
	1000			13%	0.34		
LSC	100			28%	0.83		
	200			12%	0.36		
	300			24%	0.07		
	400			32%	0.01		
	1000			19%	0.14		
DSC	100			3%	0.80		
	200			-10%	0.42		
	300			19%	0.16		
	400			30%	0.33		
	1000			8%	0.53		
NC	100			-7%	0.58		
	200			2%	0.90		
	300			2%	0.85		
	400			29%	0.03		
	1000			27%	0.03		
KMNC	100			-3%	0.83		
	200			5%	0.69		
	300			-13%	0.34		
	400			11%	0.40		
	1000			19%	0.14		
NBC	100			2%	0.88		
	200			-22%	0.09		
	300			9%	0.53		
	400			-2%	0.87		
	1000			31%	0.0006		
TKNC	100			27%	0.06		
	200			22%	0.08		
	300			17%	0.19		
	400			13%	0.31		
	1000			30%	0.02		
SNAC	100			5%	0.72		
	200			-29%	0.02		
	300			3%	0.80		
	400			-10%	0.45		
	1000			32%	0.0004		

Table 5: Correlation results between test criteria and DNN faults. The grey boxes refer to statistically significant correlations (p-value ≤ 0.05)

Dataset	Model	Metric	Test Set Size	Spearman	P-value		
MNIST	LeNet-1	GD	100	33%	0.01		
			200	39%	0.002		
			300	28%	0.04		
			400	33%	0.01		
			1000	29%	0.03		
		STD	100	6%	0.67		
			200	26%	0.04		
			300	20%	0.15		
			400	12%	0.36		
			1000	16%	0.21		
		LSC	100	-6%	0.62		
			200	23%	0.08		
			300	18%	0.19		
			400	12%	0.35		
			1000	16%	0.22		
		DSC	100	13%	0.33		
			200	-21%	0.10		
			300	-25%	0.07		
			400	17%	0.19		
			1000	6%	0.67		
		NC	100	6%	0.67		
			200	22%	0.10		
			300	24%	0.08		
			400	-6%	0.67		
			1000	3%	0.82		
		KMNC	100	22%	0.10		
			200	13%	0.32		
			300	2%	0.86		
			400	-3%	0.84		
			1000	19%	0.15		
		NBC	100	-30%	0.02		
			200	32%	0.01		
			300	20%	0.15		
			400	8%	0.52		
			1000	-13%	0.33		
		TKNC	100	10%	0.46		
			200	2%	0.89		
			300	2%	0.88		
			400	19%	0.15		
			1000	13%	0.31		
		SNAC	100	-28%	0.03		
			200	27%	0.03		
			300	25%	0.07		
			400	4%	0.76		
			1000	-13%	0.32		
		Fashion-MNIST	LeNet-4	GD	100	31%	0.02
					200	32%	0.01
					300	30%	0.02
400	26%				0.05		
1000	28%				0.03		
STD	100			10%	0.48		
	200			10%	0.43		
	300			3%	0.82		
	400			9%	0.48		
	1000			18%	0.18		
LSC	100			14%	0.31		
	200			10%	0.44		
	300			11%	0.42		
	400			9%	0.48		
	1000			7%	0.61		
DSC	100			15%	0.28		
	200			-19%	0.14		
	300			-12%	0.37		
	400			-14%	0.28		
	1000			8%	0.55		
NC	100			-6%	0.66		
	200			25%	0.06		
	300			6%	0.63		
	400			22%	0.10		
	1000			10%	0.46		
KMNC	100			18%	0.18		
	200			20%	0.13		
	300			36%	0.01		
	400			27%	0.03		
	1000			24%	0.07		
NBC	100			-0.2%	0.99		
	200			2%	0.88		
	300			15%	0.24		
	400			1%	0.93		
	1000			25%	0.06		
TKNC	100			22%	0.09		
	200			13%	0.31		
	300			18%	0.18		
	400			6%	0.66		
	1000			13%	0.32		
SNAC	100			1%	0.96		
	200			2%	0.86		
	300			16%	0.22		
	400			1%	0.95		
	1000			25%	0.06		

Table 6: Correlation results between test criteria and DNN faults. The grey boxes refer to statistically significant correlations (p-value ≤ 0.05)

Dataset	Model	Metric	Test Set Size	Spearman	P-value
Cifar-10	ResNet20	GD	100	26%	0.05
			200	31%	0.01
			300	37%	0.004
			400	29%	0.03
			1000	28%	0.03
		STD	100	16%	0.22
			200	28%	0.03
			300	34%	0.01
			400	20%	0.13
			1000	28%	0.03
		LSC	100	16%	0.24
			200	33%	0.01
			300	-10%	0.43
			400	9%	0.50
			1000	-6%	0.63
		DSC	100	-3%	0.82
			200	-14%	0.28
			300	1%	0.98
			400	9%	0.48
			1000	18%	0.16
		NC	100	12%	0.38
			200	16%	0.23
			300	-6%	0.64
			400	6%	0.66
			1000	7%	0.60
		KMNC	100	4%	0.79
			200	13%	0.32
			300	18%	0.17
			400	26%	0.05
			1000	33%	0.01
		NBC	100	13%	0.31
			200	13%	0.32
			300	15%	0.25
			400	12%	0.37
			1000	7%	0.61
		TKNC	100	-1%	0.96
			200	1%	0.95
			300	16%	0.23
			400	22%	0.10
			1000	1%	0.93
		SNAC	100	16%	0.24
			200	13%	0.34
			300	19%	0.15
			400	11%	0.40
			1000	11%	0.41

Table 7: Correlation results between test criteria and DNN faults. The grey boxes refer to statistically significant correlations (p-value ≤ 0.05)

between GD and faults in all configurations (30/30). Furthermore, they are consistent across all the studied models, datasets and input sets sizes. On the other hand, we found that STD has a positive significant correlation with faults in only ten configurations. These results were expected since, in RQ1, GD showed better performance in measuring actual data diversity than STD.

Note that we expected to have a moderate correlation between diversity and faults as we rely on a clustering approach to approximate faults in DNNs (section 3.3.1). Such correlation is expected to be higher if we had a more straightforward method to identify faults in DNNs. Nevertheless, the obtained results clearly indicate that GD can be used as guidance to effectively test DNNs by devising input sets with maximum diversity so as to increase their fault revealing capabilities. Let us recall that GD has also the practical advantage of being black-box, as opposed state-of-the-art DNN coverage metrics [12], [13], [10], [11] that require access to the internals of DNN models or their training sets.

Dataset	Model	Metric	Test Set Size	Spearman	P-value
SVHN	LeNet5	GD	100	27%	0.04
			200	27%	0.03
			300	27%	0.04
			400	33%	0.01
			1000	30%	0.02
		STD	100	27%	0.04
			200	16%	0.21
			300	20%	0.13
			400	23%	0.08
			1000	6%	0.65
		LSC	100	-5%	0.72
			200	20%	0.12
			300	10%	0.45
			400	27%	0.04
			1000	3%	0.83
		DSC	100	-17%	0.20
			200	-9%	0.50
			300	-5%	0.69
			400	4%	0.75
			1000	8%	0.57
		NC	100	9%	0.49
			200	6%	0.64
			300	-2%	0.89
			400	-6%	0.67
			1000	-6%	0.63
		KMNC	100	15%	0.25
			200	22%	0.09
			300	-2%	0.89
			400	26%	0.05
			1000	7%	0.61
		NBC	100	-6%	0.64
			200	13%	0.31
			300	16%	0.22
			400	11%	0.41
			1000	-6%	0.64
		TKNC	100	14%	0.29
			200	4%	0.77
			300	10%	0.46
			400	9%	0.50
			1000	-16%	0.23
		SNAC	100	-6%	0.64
			200	13%	0.31
			300	-16%	0.22
			400	11%	0.41
			1000	-6%	0.64

Table 8: Correlation results between test criteria and DNN faults. The grey boxes refer to statistically significant correlations (p-value ≤ 0.05)

Answer to RQ2: There is a positive and statistically significant correlation between GD and faults in DNNs. GD is much more frequently correlated to faults than STD. Consequently, GD should be used as a black-box approach to guide the testing of DNN models.

3.3.4 RQ3. How does coverage relate to fault detection?

Similar to the previous section with diversity, with this research question, we want to study the correlation between state-of-the-art coverage criteria and faults in DNNs. Our goal is to understand how they compare with diversity with that respect. We selected, based on three factors, the following two coverage criteria: Likelihood-based Surprise Coverage (LSC) and Distance-based Surprise Coverage (DSC) [10]. First, we retained criteria that have been recently published in the literature. We also chose those that (1) have been compared to other coverage criteria, and (2) showed better performance in guiding the test of DNN models. Finally, we selected the coverage metrics that we could apply and replicate on our models and datasets. The first two factors

Dataset	Model	GD	STD	LSC	DSC	NC	KMNC	NBC	TKNC	SNAC
MNIST	LeNet-1	5/5	1/5	0/5	0/5	0/5	0/5	1/5	0/5	1/5
MNIST	LeNet-5	5/5	2/5	1/5	0/5	2/5	0/5	1/5	1/5	1/5
Fashion-MNIST	LeNet-4	5/5	0/5	0/5	0/5	0/5	2/5	0/5	0/5	0/5
Cifar-10	12-layer ConvNet	5/5	3/5	0/5	0/5	0/5	0/5	0/5	3/5	0/5
Cifar-10	ResNet20	5/5	3/5	1/5	0/5	0/5	2/5	0/5	0/5	0/5
SVHN	LeNet-5	5/5	1/5	1/5	0/5	0/5	1/5	0/5	0/5	0/5
Total		30/30	10/30	3/30	0/30	2/30	5/30	2/30	4/30	2/30

Table 9: Number of positive statistically significant correlations between testing criteria and faults

yielded four coverage metrics: Likelihood-based Surprise Coverage, Distance-based Surprise Coverage, Importance-Driven Coverage (IDC) [11] and Sign-Sign Coverage (SSC) [14]. However, we could not apply IDC and SSC on our datasets and models. More precisely, we got several execution errors² when we tried to compute IDC on 12-layer ConvNet and LeNet models. Furthermore, for SSC, we obtained different results from the original paper [14] when we applied this metric on LeNet-1 and faced again several execution errors for the remaining models. Therefore, we excluded these metrics from our study and considered only LSC and DSC to study the correlation between coverage and fault detection in DNNs. In addition to the above criteria, we have also included basic and widely used criteria such as Neuron Coverage (NC) [12] and DeepGauge [13] coverage metrics. More precisely, we have considered the following metrics related to DeepGauge: k-Multisection Neuron Coverage (KMNC), Neuron Boundary Coverage (NBC), Top-K Neuron Coverage (TKNC) and Strong Neuron Activation Coverage (SNAC). For further information, we describe all these metrics and their limitations in section 6.

To investigate the relationship between coverage and fault detection, we run the same experiment as in RQ2 and consider the same selected subsets. We calculate the different coverage scores of all of them. We should note that for LSC and DSC, we used the same recommended settings for hyperparameters (e.g., upper bound, lower bound, number of buckets) as in the original paper [10] and other existing papers in the literature [53]. Furthermore, we used the same hyperparameters that have been recommended in the literature [13] for NC, KMNC and TKNC. We considered the activation threshold of 10% for NC and fixed the number of buckets K to three for TKNC and 1000 for KMNC and this is for the different models and datasets in our experiments. We calculate the Spearman correlation between each coverage criterion and the number of faults, and report the results in Tables 5, 6, 7, 8, and 9.

We considered 30 configurations per metric (6 models & datasets \times 5 input sizes). Further, we accounted for a total of 210 configurations related to the coverage criteria (6 models & datasets \times 7 criteria \times 5 input sizes). As depicted in Table 9, out of 30 different configurations per metric, the distributions of positive, statistically significant correlations to faults are as follows: 5 for KMNC, 4 for TKNC, 3 for

LSC, and 2 for NC, NBC and SNAC. DSC, however, did not show any statistically significant correlation with faults in any of the datasets and models. We conclude that, in general, significant correlations between coverage and faults are rare in the configurations of models and datasets that we have used. In other words, none of the studied coverage metrics consistently showed statistically significant correlations across all the considered models, datasets and input sets sizes. For example, we found that LSC is positively correlated to faults in only three out of 30 configurations related to LeNet-5 and ResNet20. However, we did not find any statistically significant correlation for this metric with LeNet-1, LeNet-4 and 12-layer ConvNet.

Our findings raise questions the usefulness of the selected coverage criteria for enabling effective DNN testing in terms of fault detection. These results confirm, from a different angle, many recent studies [16], [18], [52] that questioned the reliability of such coverage criteria to guide the test of DNN models. A central concern raised by these articles is about whether such coverage metrics relate to the model decision logic. Our results suggest that this relationship is at best weak.

Answer to RQ3: In general, significant positive correlations between coverage and faults are rare based on the configurations and datasets used in our experiments. Coverage metrics are not a good indicator of fault detection.

3.3.5 RQ4. How do diversity and coverage perform in terms of computation time?

We want to compare the computation times of the selected diversity metrics and coverage criteria and assess how they scale with the size of test sets. For this purpose, we randomly select, with replacement, 60 samples of size $n \in \{100, 200, 300, 400\}$. We calculated, for each sample, diversity and coverage scores, and measured their respective computation times. Since in RQ2 we found that GD outperforms STD in terms of the correlation to faults, we only consider in the rest of this work the GD metric to calculate diversity in input sets. We should note that for GD, we account for the sum of the following two computation times: (1) calculation of diversity based on the extracted features, and (2) the pre-processing time that is required to extract features with the VGG-16 model. We report in Figures 9 and 10 the change in computation times for ResNet20 and

². Authors have been contacted but the execution errors have not been resolved.

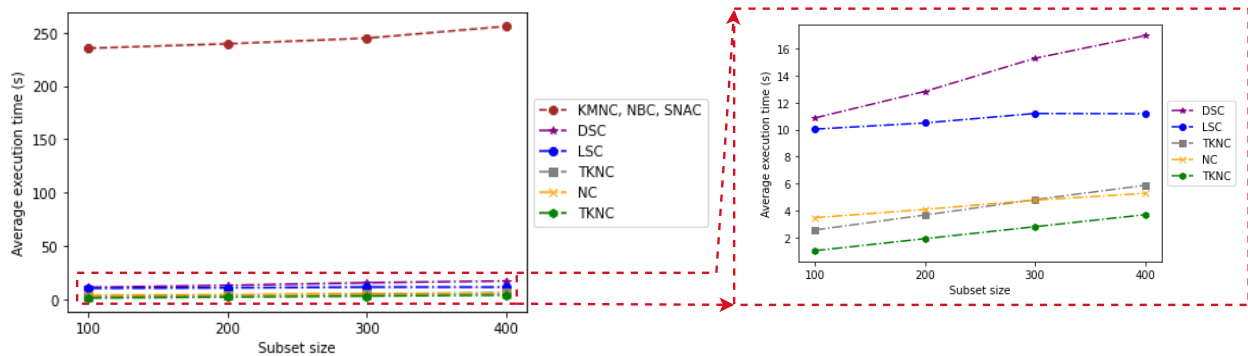


Figure 9: Computation time for diversity and coverage metrics with Cifar-10 and ResNet20

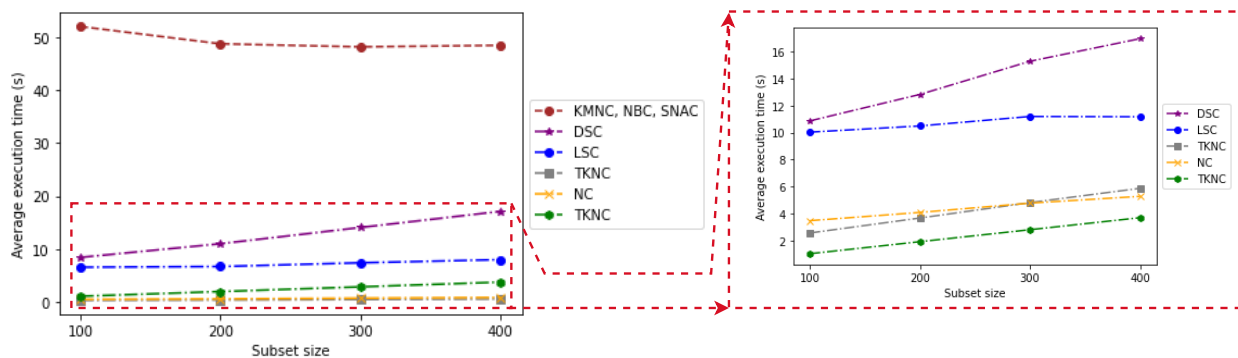


Figure 10: Computation time for diversity and coverage metrics with MNIST and LeNet-5

LeNet-5 as we increase the size of the input sets. We observe that, for both diversity and coverage metrics computation time is linear with test set sizes up to 400.

Both types of metrics are not computationally expensive. For example, the computation time related to diversity and coverage metrics in MNIST and LeNet-5 varies between 0.4 to 49 seconds for samples of size 400. We observe that KMNC, SNAC and NBC have the same computation time. Further, they are the most computationally expensive metrics. For example, KMNC, SNAC and NBC are approximately 25 times more computationally expensive than the other metrics in ResNet20. However, we found that GD generally outperforms most of the coverage metrics in terms of computation time, except NC and TKNC in LeNet-5. We use the Wilcoxon signed-rank test [71] to assess the statistical significance of the difference between the computation time of GD and the other testing criteria. We found that GD statistically outperforms all coverage metrics in terms of computation time. It is faster (about three to five times) to compute GD than LSC and DSC, for example. Though absolute differences are a matter of seconds, such computations, in the context of test selection or minimization, can be performed thousands of times and thus become practically significant. We also studied the distributions of the computation times for diversity and coverage metrics and analyzed their variations. Due to space limitation, we include the related boxplots in our replication package. We found that the distributions of the computations times related to GD show less variation than the studied coverage metrics for samples of the same size. For example, GD showed less

variation than LSC and DSC for samples of the same size. This is because the GD metric depends on the calculation of the determinant of a fixed-size feature matrix, while LSC and DSC depend on a search mechanism for the nearest inputs in the training set. Search time may vary from one sample to another and therefore leads to increased variance in computation time. Note that since GD is black-box, its computation time only depends on the used dataset and is not affected by the complexity of the DNN model (e.g., number of layers and neurons). In contrast, the computation time of white-box coverage metrics is highly sensitive to such complexity.

Answer to RQ4: Both diversity and coverage metrics are not computationally expensive. However, in general GD significantly outperforms coverage criteria. In application contexts, such as test case selection and minimization, based for example on search where we can expect to perform many test set evaluations, this difference can become practically significant.

3.3.6 RQ5. How does diversity relate to coverage?

We want to study in this research question the relationship between diversity and coverage to assess if diverse input sets tend to increase the coverage of DNN models. Conversely, increasing coverage should in theory increase diversity. Though results from previous research questions make it unlikely for such correlations to be strong, this

needs to be investigated. For this purpose, we run the same experiment as for RQ2 and RQ3 and consider the same selected subsets. We calculate, for each subset, the geometric diversity and coverage scores and measure the Spearman correlation between each pair of diversity and coverage metrics. We considered in total 175 configurations (1 diversity metric \times 7 coverage criteria \times 5 models & datasets \times 5 test set sizes). We include all the results in Appendix A and make them available online³. Out of 175 configurations, only 13 correlations were positive and statistically significant. For example, the only positive correlation (46%) between GD and LSC was for input sets of size 400 from Cifar-10 using ResNet-20. Furthermore, the only statistically significant correlation (-35%) between GD and DSC was for input sets of size 300 from Fashion-MNIST using LeNet-4. For NC, we got only three statistically significant correlations in three different models (LeNet-4, LeNet-5 and ResNet-20). Although we got six statistically significant correlations between KMNC and GD, these results were not consistent across all models and input set sizes. Additionally, the only statistically significant correlation (48%) between GD and NBC was for input sets of size 1000 from MNIST using LeNet-5. Finally, for TKNC and SNAC, we got for each metric only two statistically significant correlations with GD. To summarize, most configurations (159) show no significant correlations between diversity and coverage metrics, which suggest that, in general, diversity and coverage in DNN models are not correlated. In other words, diverse input sets do not necessarily increase the coverage of DNN models and higher coverage does not systematically lead to higher diversity. These results are also consistent with our previous observations in RQ3 and RQ4 where we found that while geometric diversity is correlated to fault detection, coverage is not.

Answer to RQ5: In general, for most configurations, there is no significant correlation between diversity and coverage in DNN models.

4 DISCUSSION AND RECOMMENDATIONS

We should note that our correlation results between testing criteria and faults are consistent across different datasets and DNN models. Based on our experiments, we show that studying the diversity of the features embedded in test input sets is more reliable to test DNNs than considering the coverage of their hidden neurons. In fact, we show that geometric diversity is potentially more effective than existing coverage metrics in guiding the test of DNN models. This metric requires neither knowledge about the model under test nor access to the training set, and is therefore a practical, black-box approach that can be used to guide the testing of DNN models. Though results are encouraging, we only studied geometric diversity with DNN models that take images as input. More experiments should be done to further assess its performance on other input data types to make our results more generalizable.

Based on our experiments, we were also surprised to see only a few significant correlations between coverage and

faults across all the models and datasets we considered. Note that we selected both widely used coverage criteria in the literature and the best coverage metrics in term of published results and reproducibility (section 3.3.4). Nevertheless coverage showed poor performance as indicators of detected faults in DNNs. In traditional software, one of the potential reasons of the effectiveness of coverage criteria is that they rely on the system’s source code logical structure. However, the decision logic in DNNs is not explicit, which makes the definition and usage of coverage criteria more challenging in the context of DNNs. Also, in traditional software, relying on diverse test cases tends to increase code coverage and the fault-detection capabilities of test suites [19], [72]. In contrast, we show that in DNN testing, diverse test input sets do not lead to increased DNN coverage but, at least for geometric diversity, lead to detecting more faults in the DNN model.

Furthermore, traditional software systems and DNNs are fundamentally different with respect to the notion of fault and their detection. Given a test input, in general, we detect faults in regular software by comparing the actual test output to the expected output. If there is a mismatch, then we consider this to be a failure and we can debug the system using various fault localization techniques [73], [74], [75] to identify faulty statement(s). However, in DNN models the notion of fault is elusive because of the black-box nature of DNN models. If the DNN model mispredicts an input, we consider this to be a failure but debugging and localising faults in the DNN causing such failure is challenging as there is no explicit and interpretable decision logic. This is also why DNNs are usually fixed through retraining [24]. Because it is common for many mispredicted inputs to be caused by the same problems in the DNN model [24], and because we cannot directly identify root causes, we relied on a clustering-based approach to group similar mispredicted inputs and thus rely on the number of such clusters to approximate fault counting in our experiments. Our clustering relies on a density-based clustering algorithm that groups similar mispredicted inputs based on their (image) features and their misprediction behaviour (pairs of actual and mispredicted classes). However, more research work is still needed to investigate alternative ways to enable fault detection comparisons in experiments involving DNN models.

To summarise, the practical implications of our results is that one should not to rely on coverage, as currently defined, to guide the testing of DNNs if the objective is to detect as many faults as possible and guide future retraining. Alternatively, we show in this paper that geometric diversity has strong potential as an alternative. It outperforms existing coverage approaches in terms of fault-revealing capability, applicability (as it is black-box) and computational time. We therefore recommend it to software developers to drive test set selection, generation and minimisation.

5 THREATS TO VALIDITY

We discuss in this section the different threats to the validity of our study and describe how we mitigated them.

Internal threats to validity concern the causal relationship between the treatment and the outcome. We have selected

3. <https://github.com/zohreh-aaa/DNN-Testing>

in our study three diversity metrics that we re-implemented since their source code was unavailable (GD and STD) or not applicable on our datasets (NCD). Consequently, an internal threat to validity might be related to our implementations. To mitigate this threat, we have carefully checked our code and its conformance with the original papers in which they were published. We have also verified the correctness of our implementation of the NCD metric by comparing our results with an existing implementation⁴ that supports the calculation of the NCD score for only pairs of images or *txt* files. We have also tested in *RQI*, through a controlled experiment, the reliability of the selected diversity metrics in measuring actual data diversity and excluded the metrics that failed the test.

As we are targeting black-box diversity metrics, we need to rely on a feature extraction model to build our feature matrix. Therefore, an internal threat to validity might be caused by low quality representation of inputs. To mitigate this threat, we have relied on VGG-16, which is one of the most used and accurate, state-of-the-art feature extraction models. Furthermore, this DNN model has been pre-trained on the extremely large ImageNet dataset, which contains over 14 million labelled images belonging to 22000 categories.

Further, the configuration of the different hyperparameters in our study may induce additional internal threats to validity. We mitigate this threat in two ways: (1) for coverage metrics hyperparameters, we make use of the original papers' hyperparameter values [10] for each dataset and model that we use, and (2) for fault estimation hyperparameters (clustering), we tried more than 500 configurations related to HDBSCAN and UMAP for each of the datasets and models that we have considered in our experiments. To reduce potential bias, we evaluated the configurations' results using two clustering evaluation metrics (section 3.3.1) and by visualising heatmaps.

A last internal threat to validity would be related to randomness when sampling test inputs. We addressed this issue by repeating such sampling multiple times while considering different input set sizes and different datasets and models.

Construct threats to validity concern the relation between the theory and the observations made. To study the effectiveness of a given test criterion in guiding DNN testing, we rely on a clustering-based approach to estimate detected faults in DNNs. It is a potential threat to construct validity as this estimate may not be sufficiently accurate. If that is the case, correlations with diversity and coverage might appear weaker than they actually are. But alternatively, relying on misprediction rates is, as discussed above, much more misleading as, in practice, many similar mispredicted inputs typically result from the same problems in the DNN model. Accounting for a large number of redundant test inputs would blur our correlation analysis, an effect we have actually observed in our study. Further, we rely on a density-based clustering algorithm that is capable of grouping similar inputs in clusters of arbitrary shapes, as opposed to other types of clustering algorithms (e.g. k-means and hierarchical clustering) which assume that clusters are convex. Next,

we cluster similar mispredicted inputs based on their (image) features and misprediction behaviour, thus relying for what semantically distinguishes images. Finally, we quantitatively and qualitatively assess the obtained clusters to ensure they group test inputs with similar characteristics.

Reliability threats to validity concern the replicability of our study results. We rely on publicly available models and datasets and provide online all the materials required to replicate our study results. This includes the set of all selected samples in the experiments and the different configurations that we used for all the selected testing criteria.

Conclusion threats to validity concern the relation between the treatment and the outcome. We relied in this study on Spearman correlation as it does not rely on any assumptions about the data set distributions and the shape of the relationships, except for the latter being monotonic.

External threats to validity concern the generalizability of our study. We mitigate this threat by using four large datasets and five widely used and architecturally different DNN models. Further, for each of our experiments, we considered many samples and input set sizes. The selected coverage metrics may not be representative of all existing coverage criteria. However, we have selected the best metrics based on their published results and our ability to reproduce their results.

6 RELATED WORK

The work presented in this paper relies on concepts related to test diversity and coverage in the context of DNN testing. Therefore, we provide in this section an overview of existing coverage metrics for DNN models. We also describe existing work making use of diversity to guide the testing of DNNs and traditional software systems.

6.1 Test Coverage Criteria for DNNs

Several coverage metrics have been proposed in the literature. The first attempt was carried out by Pei *et al.* [12] who proposed the Neuron Coverage (NC) metric for test inputs, which is defined as the proportion of activated neurons (neurons whose activation value is above the defined threshold) over all neurons when all available test inputs are supplied to a DNN. However, several studies [14], [15] have shown that 100% neuron coverage is easy to achieve with a small set of inputs, thus considerably limiting the applicability of such metric when testing DNNs.

Ma *et al.* [13] proposed DeepGauge, a set of coverage metrics for DNNs. They introduced k-Multisection Neuron Coverage (KMNC), Neuron Boundary Coverage (NBC), and Strong Neuron Activation Coverage (SNAC). KMNC partitions the ranges of neuron activation values into K buckets based on training inputs and counts the number of total covered buckets by a given test input set. NBC measures the ratio of corner-case regions that have been covered. Corner-case regions correspond to the activation values that are beyond the activation ranges observed during training. Finally, SNAC measures how many upper corner-cases have been covered. Upper corner-cases correspond to neuron activation values that are greater than the activation ranges observed during training. The authors showed that input test generated by adversarial methods increase coverage in terms of their metrics. However, they did not study how

4. <https://github.com/simonpoulding/DataGenerators.jl>

these metrics relate to DNN mispredictions using natural inputs.

Inspired by the MC/DC test coverage in traditional software testing, Sun *et al.* [14] proposed four coverage metrics that take into consideration the causal relationship between neurons in neighbouring layers of a DNN model. These metrics were used to guide the generation of test inputs using adversarial methods to test the robustness of DNN models.

Kim *et al.* [10] proposed two coverage criteria called Likelihood-based Surprise Coverage (LSC) and Distance-based Surprise Coverage (DSC). These criteria are based on the analysis of how surprising test sets are given the training set. LSC uses Kernel Density Estimation (KDE) [76] to estimate the likelihood of seeing a test input during the training phase. On the other hand, DSC relies on the calculation of Euclidean distances between vectors that correspond to (1) the neurons activation values of inputs from the test set, and (2) the neurons activation values of inputs from the training set. They argue that an input set that covers a wide and diverse range of surprise values is preferable to test and retrain a DNN model. They show that their metrics are correlated with existing coverage criteria [12], [13] when the diversity of inputs is increased. However, our study shows that there is no strong correlation between surprise adequacy coverage and diversity by using only natural inputs. We also show that there is no strong correlation between these coverage metrics and faults in DNNs. Another study conducted by Chen *et al.* [18] showed similar results with respect to DNN misprediction rates when using only natural inputs.

Gerasimou *et al.* [11] proposed the Importance-Driven Coverage (IDC) criterion to focus on the coverage of the most influential neurons in DNN predictions. They argue that IDC is sensitive to adversarial inputs and achieves higher values when applied on input sets that comprise diverse inputs. They also considered DeepGauge [10] and surprise adequacy coverage criteria [13] in their experiments and observed that IDC shows a similar increase to these coverage criteria when evaluated with test sets augmented with adversarial inputs.

Despite very active research on DNN coverage, several recent articles have questioned the usefulness of coverage criteria to guide the test of DNN models [16], [17], [18]. For example, Li *et al.* [16] studied a number of structural coverage criteria and discussed their limitations in terms of fault detection capabilities in DNN models. Their experiments found no strong correlation between coverage and the number of misclassified inputs in a natural test set. Furthermore, Dong *et al.* [17] found that retraining DNN models with new input sets that improve coverage does not help increase the robustness of the model to adversarial attacks.

Our work on diversity metrics is orthogonal to existing research regarding the test coverage of DNNs. All state-of-the-art coverage metrics require full access to the internals of DNN state or training data, both of which are often not available to testers in practical contexts. Thus, in our approach we focus on black-box diversity metrics, aiming at providing guidance to assess test suites or select test cases for DNNs.

State-of-the-art coverage criteria have been largely validated with artificial inputs generated based on adversarial methods [12], [13], [14], [10], [11]. However, their relationship with (often unrealistic) adversarial inputs does not necessarily mean that they relate to the fault detection capability of natural test input sets. In fact, Li *et al.* [16] argue that adversarial inputs are pervasively distributed over the divided space defined by existing coverage criteria. On the other hand, misclassified natural inputs have a sparse distribution making their detection much more difficult when using such coverage criteria [16]. Existing studies [16], [18] have failed to find a significant correlation between coverage and the number of misclassified inputs in a test set. Consequently, coverage criteria may be ineffective at guiding the test of DNNs to increase the fault-detection capability of natural input sets.

Furthermore, existing studies [12], [13], [14], [10], [11] have used the number of mispredicted inputs to study the effectiveness of coverage criteria to support DNN testing. However, as we have discussed above, simply comparing mispredictions is highly misleading as many test inputs may (and usually do) fail due to the same causes in the DNN model. To address this problem, in our work, we approximate faults (i.e., common misprediction causes) relying in a clustering strategy and study the correlation between test criteria (i.e. coverage and diversity) and faults instead of misprediction rates.

6.2 Diversity in Testing

We will describe in the following existing work that relied on diversity to test DNNs and regular software.

Diversity in DNN Testing. A very recent study of Langford and Cheng [77] proposed Enki, a DNN input generation approach based on evolutionary search [78]. Their goal is to diversify image transformation types with the objective to generate new inputs from existing ones to test and retrain DNN models. They start by evolving an archive of image transformation types that have a diverse impact on the DNN model. Given a subset of synthetic inputs generated with a certain image transformation type, diversity of the impact is evaluated with three elements: (1) the F1-score of the DNN model when applied on the subset, (2) the neuron coverage score [12] and (3) the neurons activation pattern [77]. After building the final Enki archive that contains the most diverse image transformation types, they (1) test the DNN models using synthetic inputs generated with the identified image transformation types, and (2) study the accuracy of the DNNs by retraining it with such synthetic training data. They also compare their results with random inputs generation and DeepTest [79]. They conclude that Enki outperforms these two inputs generation approaches and report that testing DNNs with their generated data leads to the lowest DNN model accuracy. They also report that retraining DNNs with their generated data increases the accuracy of DNN models.

What differentiates our work from Enki is that the latter provides a search-based approach to diversify image transformation types, with the goal of minimizing the model accuracy, that are then used to guide the generation of synthetic inputs to test and retrain DNNs. In contrast, our approach investigates ways to measure diversity in natural

test input sets and compare the best diversity metric with state-of-the-art coverage criteria to guide DNN testing into maximizing fault detection. Such diversity metric can then be used for multiple purposes such as test suite assessment and guidance for selection, minimization, and generation. Our focus on faults, as opposed to accuracy, aims at finding test inputs whose mispredictions result from distinct root causes. For practical reasons, as already discussed and as opposed to Enki, we intentionally devise an approach that is black-box and does not rely on internal information about the model or its training set.

Diversity in Software Testing. Input and output diversity has been investigated to support different aspects related to traditional software testing. Since executing similar test cases tends to exercise similar parts of the source code, this is likely to lead to revealing the same faults in the system under test. Therefore, relying on diverse test cases should increase the exploration of the fault space and thus increase fault detection rates [80], [20], [81].

Feldt *et al.* [21] proposed Test Set Diameter (TDSm), a diversity-based test case selection strategy. The approach uses the NCD metric to measure the diversity of test inputs. They applied their approach on four systems and concluded that diverse test input sets increase code coverage. Finally, they show that test sets with larger NCD scores exhibit better fault-detection capabilities.

Hemmati *et al.* [82] conducted an empirical study on similarity-based test selection techniques for test cases generated from state machine models. They studied and compared over 320 variants that rely on different similarity metrics and selection algorithms. Based on their experiments, they found that the best test selection techniques uses the Gower-Legendre similarity function [83] and applies an (1+1) Evolutionary Algorithm [84] to select tests with minimum pairwise similarity and thus maximize the diversity of the selected test cases. They further showed that such similarity-based test selection configuration outperforms random selection and coverage-based techniques in terms of fault detection rates and computational cost.

Biagiola *et al.* [19] introduced a web test generation algorithm that produces and selects candidate test cases that will be executed in the browser based on their diversity. They show that their test generation technique achieve higher code coverage and fault detection rates when compared to state-of-the-art, search-based web test generators [72], [85].

Our objectives in this paper are similar to the above works but in the context of DNN testing. As several studies have shown the effectiveness of diversity metrics to guide the testing of software systems, we investigate in this paper its usefulness in testing DNN models. We therefore compare the performance of existing diversity metrics with state-of-the-art DNNs coverage criteria in terms of their fault detection capabilities and computational cost.

7 CONCLUSION

In this paper, we study the effectiveness of input diversity metrics in guiding the testing of DNN models. We focus on DNN models using images as inputs, as they are very common in many systems. Our motivation is to provide a black-box mechanism, not relying on DNN internal information or training data, to assess test sets. Such requirement

aims at making our approach more applicable in the many practical contexts where such information is not (easily) accessible. We also compare the results achieved by white-box coverage criteria defined for DNNs with those of black-box diversity.

To this end, we selected and adapted three diversity metrics and, by means of a controlled experiment, evaluated their capability to measure actual input diversity. We selected the best metrics and analysed their association with fault detection in DNNs using four datasets and five DNN models. Because simply comparing mispredictions is highly misleading, as many test inputs fail for the same reasons, and because we cannot directly identify root causes of mispredictions in DNNs, we relied on a clustering-based approach to group similar mispredicted inputs and thus estimated faults based on the number of such clusters. We further selected the best state-of-the-art coverage criteria based on published results and our ability to reproduce their published results. We studied the associations of the selected coverage criteria with both diversity and fault detection.

Based on our experiments, we found that the best diversity metric is geometric diversity and that, though there is still room for improvement, it is far more effective than the selected coverage criteria in guiding the testing of DNN models. This metric outperforms these coverage criteria in terms of fault-revealing capability and computational time. We therefore conclude that geometric diversity is a good black-box option to guide the testing of DNN models using images as inputs. We aim to extend our work by studying the application of input diversity in supporting different testing scenarios such as test set selection, minimisation and generation.

ACKNOWLEDGEMENTS

We are grateful to Kim *et al.* [10] for their help and support to replicate the surprise adequacy coverage results. This work was supported by a research grant from General Motors as well as the Canada Research Chair and Discovery Grant programs of the Natural Sciences and Engineering Research Council of Canada (NSERC).

REFERENCES

- [1] X. Yang, F. Li, and H. Liu, "A survey of dnn methods for blind image quality assessment," *IEEE Access*, vol. 7, pp. 123 788–123 806, 2019.
- [2] A. Giusti, D. C. Cireşan, J. Masci, L. M. Gambardella, and J. Schmidhuber, "Fast image scanning with deep max-pooling convolutional neural networks," in *2013 IEEE International Conference on Image Processing*. IEEE, 2013, pp. 4034–4038.
- [3] P. K. Mallick, S. H. Ryu, S. K. Satapathy, S. Mishra, G. N. Nguyen, and P. Tiwari, "Brain mri image classification for cancer detection using deep wavelet autoencoder-based deep neural network," *IEEE Access*, vol. 7, pp. 46 278–46 287, 2019.
- [4] V. Rajinikanth, A. N. Joseph Raj, K. P. Thanaraj, and G. R. Naik, "A customized vgg19 network with concatenation of deep and handcrafted features for brain tumor detection," *Applied Sciences*, vol. 10, no. 10, p. 3429, 2020.
- [5] T. G. Debelee, S. R. Kebede, F. Schwenker, and Z. M. Shewarega, "Deep learning in selected cancers' image analysis—a survey," *Journal of Imaging*, vol. 6, no. 11, p. 121, 2020.
- [6] J. Pan, C. Liu, Z. Wang, Y. Hu, and H. Jiang, "Investigation of deep neural networks (dnn) for large vocabulary continuous speech recognition: Why dnn surpasses gmms in acoustic modeling," in *2012 8th International Symposium on Chinese Spoken Language Processing*. IEEE, 2012, pp. 301–305.

- [7] A. E. Sallab, M. Abdou, E. Perot, and S. Yogamani, "Deep reinforcement learning framework for autonomous driving," *Electronic Imaging*, vol. 2017, no. 19, pp. 70–76, 2017.
- [8] A. Stocco, M. Weiss, M. Calzana, and P. Tonella, "Misbehaviour prediction for autonomous driving systems," in *Proceedings of the ACM/IEEE 42nd International Conference on Software Engineering*, 2020, pp. 359–371.
- [9] X. Cai and M. R. Lyu, "The effect of code coverage on fault detection under different testing profiles," in *Proceedings of the 1st International Workshop on Advances in Model-based Testing*, 2005, pp. 1–7.
- [10] J. Kim, R. Feldt, and S. Yoo, "Guiding deep learning system testing using surprise adequacy," in *2019 IEEE/ACM 41st International Conference on Software Engineering (ICSE)*. IEEE, 2019, pp. 1039–1049.
- [11] S. Gerasimou, H. F. Eniser, A. Sen, and A. Cakan, "Importance-driven deep learning system testing," in *2020 IEEE/ACM 42nd International Conference on Software Engineering (ICSE)*. IEEE, 2020, pp. 702–713.
- [12] K. Pei, Y. Cao, J. Yang, and S. Jana, "Deepxplore: Automated whitebox testing of deep learning systems," in *proceedings of the 26th Symposium on Operating Systems Principles*, 2017, pp. 1–18.
- [13] L. Ma, F. Juefei-Xu, F. Zhang, J. Sun, M. Xue, B. Li, C. Chen, T. Su, L. Li, Y. Liu, J. Zhao, and Y. Wang, "Deepgauge: Multi-granularity testing criteria for deep learning systems," *2018 33rd IEEE/ACM International Conference on Automated Software Engineering (ASE)*, pp. 120–131, 2018.
- [14] Y. Sun, X. Huang, D. Kroening, J. Sharp, M. Hill, and R. Ashmore, "Structural test coverage criteria for deep neural networks," *ACM Transactions on Embedded Computing Systems (TECS)*, vol. 18, no. 5s, pp. 1–23, 2019.
- [15] J. Sekhon and C. Fleming, "Towards improved testing for deep learning," in *2019 IEEE/ACM 41st International Conference on Software Engineering: New Ideas and Emerging Results (ICSE-NIER)*. IEEE, 2019, pp. 85–88.
- [16] Z. Li, X. Ma, C. Xu, and C. Cao, "Structural coverage criteria for neural networks could be misleading," in *2019 IEEE/ACM 41st International Conference on Software Engineering: New Ideas and Emerging Results (ICSE-NIER)*. IEEE, 2019, pp. 89–92.
- [17] Y. Dong, P. Zhang, J. Wang, S. Liu, J. Sun, J. Hao, X. Wang, L. Wang, J. Dong, and T. Dai, "An empirical study on correlation between coverage and robustness for deep neural networks," in *2020 25th International Conference on Engineering of Complex Computer Systems (ICECCS)*. IEEE, 2020, pp. 73–82.
- [18] J. Chen, M. Yan, Z. Wang, Y. Kang, and Z. Wu, "Deep neural network test coverage: How far are we?" *arXiv preprint arXiv:2010.04946*, 2020.
- [19] M. Biagiola, A. Stocco, F. Ricca, and P. Tonella, "Diversity-based web test generation," in *Proceedings of the 2019 27th ACM Joint Meeting on European Software Engineering Conference and Symposium on the Foundations of Software Engineering*, 2019, pp. 142–153.
- [20] H. Hemmati, Z. Fang, and M. V. Mantyla, "Prioritizing manual test cases in traditional and rapid release environments," in *2015 IEEE 8th International Conference on Software Testing, Verification and Validation (ICST)*. IEEE, 2015, pp. 1–10.
- [21] R. Feldt, S. Poulding, D. Clark, and S. Yoo, "Test set diameter: Quantifying the diversity of sets of test cases," in *2016 IEEE International Conference on Software Testing, Verification and Validation (ICST)*. IEEE, 2016, pp. 223–233.
- [22] T. Y. Chen, F.-C. Kuo, R. G. Merkel, and T. Tse, "Adaptive random testing: The art of test case diversity," *Journal of Systems and Software*, vol. 83, no. 1, pp. 60–66, 2010.
- [23] T. Y. Chen, R. Merkel, P. Wong, and G. Eddy, "Adaptive random testing through dynamic partitioning," in *Fourth International Conference on Quality Software, 2004. QSI 2004. Proceedings*. IEEE, 2004, pp. 79–86.
- [24] H. Fahmy, F. Pastore, M. Bagherzadeh, and L. Briand, "Supporting deep neural network safety analysis and retraining through heatmap-based unsupervised learning," *IEEE Transactions on Reliability*, 2021.
- [25] A. Kulesza and B. Taskar, "Determinantal point processes for machine learning," *arXiv preprint arXiv:1207.6083*, 2012.
- [26] K. Simonyan and A. Zisserman, "Very deep convolutional networks for large-scale image recognition," *arXiv preprint arXiv:1409.1556*, 2014.
- [27] W. Mousser and S. Ouadfel, "Deep feature extraction for pap-smear image classification: A comparative study," in *Proceedings of the 2019 5th International Conference on Computer and Technology Applications*, 2019, pp. 6–10.
- [28] T. Kaur and T. K. Gandhi, "Automated brain image classification based on vgg-16 and transfer learning," in *2019 International Conference on Information Technology (ICIT)*. IEEE, 2019, pp. 94–98.
- [29] Z. Gong, P. Zhong, and W. Hu, "Diversity in machine learning," *IEEE Access*, vol. 7, pp. 64 323–64 350, 2019.
- [30] A. R. Cohen and P. M. Vitányi, "Normalized compression distance of multisets with applications," *IEEE transactions on pattern analysis and machine intelligence*, vol. 37, no. 8, pp. 1602–1614, 2014.
- [31] H. Lin and J. A. Bilmes, "Learning mixtures of submodular shells with application to document summarization," *arXiv preprint arXiv:1210.4871*, 2012.
- [32] B. Kang, "Fast determinantal point process sampling with application to clustering," *Advances in Neural Information Processing Systems*, vol. 26, 2013.
- [33] H. Xu and Z. Ou, "Scalable discovery of audio fingerprint motifs in broadcast streams with determinantal point process based motif clustering," *IEEE/ACM Transactions on Audio, Speech, and Language Processing*, vol. 24, no. 5, pp. 978–989, 2016.
- [34] H. Z. Nafchi, A. Shahkolaei, R. Hedjam, and M. Cheriet, "Mean deviation similarity index: Efficient and reliable full-reference image quality evaluator," *Ieee Access*, vol. 4, pp. 5579–5590, 2016.
- [35] R. S. Borbely, "On normalized compression distance and large malware," *Journal of Computer Virology and Hacking Techniques*, vol. 12, no. 4, pp. 235–242, 2016.
- [36] R. Cilibrasi and P. M. Vitányi, "Clustering by compression," *IEEE Transactions on Information theory*, vol. 51, no. 4, pp. 1523–1545, 2005.
- [37] M. Elfeki, C. Couprie, M. Riviere, and M. Elhoseiny, "Gdpp: Learning diverse generations using determinantal point processes," in *International Conference on Machine Learning*. PMLR, 2019, pp. 1774–1783.
- [38] B. Gong, W.-L. Chao, K. Grauman, and F. Sha, "Diverse sequential subset selection for supervised video summarization," *Advances in neural information processing systems*, vol. 27, pp. 2069–2077, 2014.
- [39] T. Zhou, Z. Kuscsik, J.-G. Liu, M. Medo, J. R. Wakeling, and Y.-C. Zhang, "Solving the apparent diversity-accuracy dilemma of recommender systems," *Proceedings of the National Academy of Sciences*, vol. 107, no. 10, pp. 4511–4515, 2010.
- [40] A. Krause, A. Singh, and C. Guestrin, "Near-optimal sensor placements in gaussian processes: Theory, efficient algorithms and empirical studies," *Journal of Machine Learning Research*, vol. 9, no. 2, 2008.
- [41] E. Celis, V. Keswani, D. Straszak, A. Deshpande, T. Kathuria, and N. Vishnoi, "Fair and diverse dpp-based data summarization," in *International Conference on Machine Learning*. PMLR, 2018, pp. 716–725.
- [42] Y. Bengio, G. Mesnil, Y. Dauphin, and S. Rifai, "Better mixing via deep representations," in *International conference on machine learning*. PMLR, 2013, pp. 552–560.
- [43] A. N. Kolmogorov, "Three approaches to the quantitative definition of information," *Problems of information transmission*, vol. 1, no. 1, pp. 1–7, 1965.
- [44] C. H. Bennett, P. Gács, M. Li, P. M. Vitányi, and W. H. Zurek, "Information distance," *IEEE Transactions on information theory*, vol. 44, no. 4, pp. 1407–1423, 1998.
- [45] M. Li, X. Chen, X. Li, B. Ma, and P. M. Vitányi, "The similarity metric," *IEEE transactions on Information Theory*, vol. 50, no. 12, pp. 3250–3264, 2004.
- [46] R. Feldt, R. Torkar, T. Gorschek, and W. Afzal, "Searching for cognitively diverse tests: Towards universal test diversity metrics," in *2008 IEEE International Conference on Software Testing Verification and Validation Workshop*. IEEE, 2008, pp. 178–186.
- [47] D. Coltuc, M. Datcu, and D. Coltuc, "On the use of normalized compression distances for image similarity detection," *Entropy*, vol. 20, no. 2, p. 99, 2018.
- [48] A. Kocsor, A. Kertész-Farkas, L. Kaján, and S. Pongor, "Application of compression-based distance measures to protein sequence classification: a methodological study," *Bioinformatics*, vol. 22, no. 4, pp. 407–412, 2006.
- [49] C. Henard, M. Papadakis, M. Harman, Y. Jia, and Y. Le Traon, "Comparing white-box and black-box test prioritization," in *2016 IEEE/ACM 38th International Conference on Software Engineering (ICSE)*. IEEE, 2016, pp. 523–534.

- [50] P. M. Bueno, W. E. Wong, and M. Jino, "Improving random test sets using the diversity oriented test data generation," in *Proceedings of the 2nd international workshop on Random testing: co-located with the 22nd IEEE/ACM International Conference on Automated Software Engineering (ASE 2007)*, 2007, pp. 10–17.
- [51] D. Leon and A. Podgurski, "A comparison of coverage-based and distribution-based techniques for filtering and prioritizing test cases," in *14th International Symposium on Software Reliability Engineering, 2003. ISSRE 2003. IEEE, 2003*, pp. 442–453.
- [52] F. Harel-Canada, L. Wang, M. A. Gulzar, Q. Gu, and M. Kim, "Is neuron coverage a meaningful measure for testing deep neural networks?" in *Proceedings of the 28th ACM Joint Meeting on European Software Engineering Conference and Symposium on the Foundations of Software Engineering, 2020*, pp. 851–862.
- [53] S. Yan, G. Tao, X. Liu, J. Zhai, S. Ma, L. Xu, and X. Zhang, "Correlations between deep neural network model coverage criteria and model quality," in *Proceedings of the 28th ACM Joint Meeting on European Software Engineering Conference and Symposium on the Foundations of Software Engineering, 2020*, pp. 775–787.
- [54] K. Alex, N. Vinod, and H. Geoffrey. The cifar-10 dataset. [Online]. Available: <http://www.cs.toronto.edu/kriz/cifar.html>
- [55] L. Deng, "The mnist database of handwritten digit images for machine learning research [best of the web]," *IEEE Signal Processing Magazine*, vol. 29, no. 6, pp. 141–142, 2012.
- [56] Y. Netzer, T. Wang, A. Coates, A. Bissacco, B. Wu, and A. Y. Ng, "Reading digits in natural images with unsupervised feature learning," 2011.
- [57] T. Zohdinasab, V. Riccio, A. Gambi, and P. Tonella, "Deephyperion: exploring the feature space of deep learning-based systems through illumination search," in *Proceedings of the 30th ACM SIGSOFT International Symposium on Software Testing and Analysis, 2021*, pp. 79–90.
- [58] M. O. Attaoui, H. Fahmy, F. Pastore, and L. Briand, "Black-box safety analysis and retraining of dnns based on feature extraction and clustering," *arXiv preprint arXiv:2201.05077*, 2022.
- [59] M. Joswiak, Y. Peng, I. Castillo, and L. H. Chiang, "Dimensionality reduction for visualizing industrial chemical process data," *Control Engineering Practice*, vol. 93, p. 104189, 2019.
- [60] L. McInnes, J. Healy, and J. Melville, "Umap: Uniform manifold approximation and projection for dimension reduction," *arXiv preprint arXiv:1802.03426*, 2018.
- [61] A. Diaz-Papkovich, L. Anderson-Trocmé, and S. Gravel, "A review of umap in population genetics," *Journal of Human Genetics*, vol. 66, no. 1, pp. 85–91, 2021.
- [62] Y. Hozumi, R. Wang, C. Yin, and G.-W. Wei, "Umap-assisted k-means clustering of large-scale sars-cov-2 mutation datasets," *Computers in biology and medicine*, vol. 131, p. 104264, 2021.
- [63] I. T. Jolliffe and J. Cadima, "Principal component analysis: a review and recent developments," *Philosophical Transactions of the Royal Society A: Mathematical, Physical and Engineering Sciences*, vol. 374, no. 2065, p. 20150202, 2016.
- [64] L. Van der Maaten and G. Hinton, "Visualizing data using t-sne." *Journal of machine learning research*, vol. 9, no. 11, 2008.
- [65] L. McInnes, J. Healy, and S. Astels, "hdbscan: Hierarchical density based clustering," *Journal of Open Source Software*, vol. 2, no. 11, p. 205, 2017.
- [66] P. J. Rousseeuw, "Silhouettes: a graphical aid to the interpretation and validation of cluster analysis," *Journal of computational and applied mathematics*, vol. 20, pp. 53–65, 1987.
- [67] D. Moulavi, P. A. Jaskowiak, R. J. Campello, A. Zimek, and J. Sander, "Density-based clustering validation," in *Proceedings of the 2014 SIAM international conference on data mining. SIAM, 2014*, pp. 839–847.
- [68] M. Ester, H.-P. Kriegel, J. Sander, and X. Xu, "Density-connected sets and their application for trend detection in spatial databases." in *KDD*, vol. 97, 1997, pp. 10–15.
- [69] Q. Hu, Y. Guo*, M. Cordy, X. Xie, L. Ma, M. Papadakis, and Y. Le Traon, "An empirical study on data distribution-aware test selection for deep learning enhancement," *ACM Transactions on Software Engineering and Methodology*, 2022.
- [70] D. G. Bonett and T. A. Wright, "Sample size requirements for estimating pearson, kendall and spearman correlations," *Psychometrika*, vol. 65, no. 1, pp. 23–28, 2000.
- [71] R. F. Woolson, "Wilcoxon signed-rank test," *Wiley encyclopedia of clinical trials*, pp. 1–3, 2007.
- [72] M. Biagiola, F. Ricca, and P. Tonella, "Search based path and input data generation for web application testing," in *International Symposium on Search Based Software Engineering. Springer, 2017*, pp. 18–32.
- [73] D. Zou, J. Liang, Y. Xiong, M. D. Ernst, and L. Zhang, "An empirical study of fault localization families and their combinations," *IEEE Transactions on Software Engineering*, 2019.
- [74] S. Pearson, J. Campos, R. Just, G. Fraser, R. Abreu, M. D. Ernst, D. Pang, and B. Keller, "Evaluating and improving fault localization," in *2017 IEEE/ACM 39th International Conference on Software Engineering (ICSE). IEEE, 2017*, pp. 609–620.
- [75] W. E. Wong, V. Debroy, R. Gao, and Y. Li, "The dstar method for effective software fault localization," *IEEE Transactions on Reliability*, vol. 63, no. 1, pp. 290–308, 2013.
- [76] M. P. Wand and M. C. Jones, *Kernel smoothing*. CRC press, 1994.
- [77] M. A. Langford and B. H. Cheng, "Enki: A diversity-driven approach to test and train robust learning-enabled systems," *ACM Transactions on Autonomous and Adaptive Systems (TAAS)*, vol. 15, no. 2, pp. 1–32, 2021.
- [78] A. E. Eiben, J. E. Smith et al., *Introduction to evolutionary computing*. Springer, 2003, vol. 53.
- [79] Y. Tian, K. Pei, S. Jana, and B. Ray, "Deepest: Automated testing of deep-neural-network-driven autonomous cars," in *Proceedings of the 40th International Conference on Software Engineering*, ser. ICSE '18. New York, NY, USA: Association for Computing Machinery, 2018, p. 303–314. [Online]. Available: <https://doi.org/10.1145/3180155.3180220>
- [80] E. G. Cartaxo, P. D. Machado, and F. G. O. Neto, "On the use of a similarity function for test case selection in the context of model-based testing," *Software Testing, Verification and Reliability*, vol. 21, no. 2, pp. 75–100, 2011.
- [81] F. G. de Oliveira Neto, A. Ahmad, O. Leifler, K. Sandahl, and E. Enouï, "Improving continuous integration with similarity-based test case selection," in *Proceedings of the 13th International Workshop on Automation of Software Test, 2018*, pp. 39–45.
- [82] H. Hemmati, A. Arcuri, and L. Briand, "Achieving scalable model-based testing through test case diversity," *ACM Transactions on Software Engineering and Methodology (TOSEM)*, vol. 22, no. 1, pp. 1–42, 2013.
- [83] R. Xu and D. Wunsch, "Survey of clustering algorithms," *IEEE Transactions on neural networks*, vol. 16, no. 3, pp. 645–678, 2005.
- [84] S. Drost, T. Jansen, and I. Wegener, "On the analysis of the (1+1) evolutionary algorithm," *Theoretical Computer Science*, vol. 276, no. 1-2, pp. 51–81, 2002.
- [85] A. Mesbah, A. Van Deursen, and D. Roest, "Invariant-based automatic testing of modern web applications," *IEEE Transactions on Software Engineering*, vol. 38, no. 1, pp. 35–53, 2011.

APPENDIX A

CORRELATION RESULTS BETWEEN GEOMETRIC DIVERSITY AND COVERAGE METRICS

Note that the grey boxes in all the following tables refer to statistically significant correlations ($p\text{-value} \leq 0.05$)

Dataset	Model	Metric	Test Set Size	Spearman	P-value
Cifar-10	12-layer ConvNet	GD & LSC	100	13%	0.45
			200	-2%	0.92
			300	1%	0.97
			400	-10%	0.58
			1000	-12%	0.53
		GD & DSC	100	-20%	0.27
			200	-11%	0.55
			300	11%	0.49
			400	-17%	0.36
			1000	-7%	0.73
		GD & NC	100	-30%	0.09
			200	12%	0.49
			300	10%	0.56
			400	2%	0.90
			1000	2%	0.91
		GD & KMNC	100	44%	0.01
			200	15%	0.40
			300	15%	0.37
			400	9%	0.63
			1000	12%	0.54
		GD & NBC	100	31%	0.08
			200	6%	0.75
			300	17%	0.31
			400	-10%	0.62
			1000	-28%	0.14
		GD & TKNC	100	-19%	0.30
			200	17%	0.33
			300	-4%	0.83
			400	7%	0.69
			1000	7%	0.71
		GD & SNAC	100	34%	0.05
			200	6%	0.75
			300	13%	0.44
			400	-13%	0.47
			1000	-28%	0.14

Table 10: Correlation results between GD and coverage metrics using 12-layer ConvNet and Cifar-10.

Dataset	Model	Metric	Test Set Size	Spearman	P-value
MNIST	LeNet-1	GD & LSC	100	-6%	0.78
			200	-12%	0.57
			300	-6%	0.78
			400	15%	0.30
			1000	-4%	0.80
		GD & DSC	100	-27%	0.17
			200	-10%	0.64
			300	-27%	0.17
			400	25%	0.09
			1000	-14%	0.41
		GD & NC	100	18%	0.38
			200	-15%	0.47
			300	3%	0.89
			400	-3%	0.85
			1000	-30%	0.08
		GD & KMNC	100	-15%	0.47
			200	-16%	0.45
			300	8%	0.68
			400	28%	0.06
			1000	6%	0.71
		GD & NBC	100	6%	0.78
			200	6%	0.79
			300	-9%	0.65
			400	15%	0.30
			1000	-15%	0.39
		GD & TKNC	100	7%	0.73
			200	11%	0.61
			300	29%	0.14
			400	21%	0.16
			1000	21%	0.23
		GD & SNAC	100	-6%	0.78
			200	7%	0.75
			300	-14%	0.47
			400	17%	0.26
			1000	-13%	0.45

Table 11: Correlation results between GD and coverage metrics using LeNet-1 and MNIST.

Dataset	Model	Metric	Test Set Size	Spearman	P-value
MNIST	LeNet-5	GD & LSC	100	3%	0.88
			200	25%	0.17
			300	26%	0.26
			400	-22%	0.23
			1000	-7%	0.74
		GD & DSC	100	13%	0.52
			200	-10%	0.59
			300	-22%	0.34
			400	5%	0.81
			1000	-1%	0.95
		GD & NC	100	-22%	0.28
			200	-11%	0.57
			300	-4%	0.86
			400	-34%	0.06
			1000	39%	0.05
		GD & KMNC	100	-1%	0.94
			200	20%	0.29
			300	4%	0.88
			400	5%	0.79
			1000	-31%	0.11
		GD & NBC	100	-27%	0.17
			200	-1%	0.95
			300	-4%	0.86
			400	-14%	0.46
			1000	48%	0.01
		GD & TKNC	100	4%	0.84
			200	24%	0.18
			300	-17%	0.46
			400	-2%	0.90
			1000	3%	0.90
		GD & SNAC	100	-18%	0.38
			200	-1%	0.95
			300	-5%	0.81
			400	-21%	0.25
			1000	41%	0.03

Table 12: Correlation results between GD and coverage metrics using LeNet-5 and MNIST.

Dataset	Model	Metric	Test Set Size	Spearman	P-value
Fashion-MNIST	LeNet-4	GD & LSC	100	0.2%	0.99
			200	28%	0.17
			300	19%	0.29
			400	21%	0.20
			1000	2%	0.94
		GD & DSC	100	17%	0.38
			200	-7%	0.73
			300	-35%	0.05
			400	-2%	0.90
			1000	2%	0.93
		GD & NC	100	-37%	0.04
			200	0.3%	0.99
			300	-5%	0.77
			400	23%	0.16
			1000	-14%	0.49
		GD & KMNC	100	23%	0.22
			200	30%	0.14
			300	33%	0.06
			400	64%	0.0001
			1000	6%	0.76
		GD & NBC	100	-25%	0.19
			200	-31%	0.13
			300	12%	0.51
			400	-22%	0.19
			1000	-21%	0.31
		GD & TKNC	100	-1%	0.95
			200	41%	0.04
			300	-3%	0.85
			400	24%	0.15
			1000	11%	0.61
		GD & SNAC	100	-25%	0.19
			200	-31%	0.13
			300	12%	0.52
			400	-21%	0.20
			1000	-19%	0.35

Table 13: Correlation results between GD and coverage metrics using LeNet-4 and Fashion-MNIST.

Dataset	Model	Metric	Test Set Size	Spearman	P-value
Cifar-10	ResNet-20	GD & LSC	100	19 %	0.31
			200	14%	0.55
			300	39%	0.11
			400	46%	0.02
			1000	-26%	0.18
		GD & DSC	100	4 %	0.85
			200	-8%	0.74
			300	5%	0.84
			400	-10%	0.65
			1000	-3%	0.86
		GD & NC	100	5 %	0.81
			200	26%	0.25
			300	-2%	0.94
			400	12%	0.58
			1000	-38%	0.04
		GD & KMNC	100	19 %	0.3
			200	39%	0.08
			300	17%	0.51
			400	41%	0.05
			1000	28%	0.15
		GD & NBC	100	24 %	0.20
			200	12%	0.60
			300	-4%	0.87
			400	-9%	0.67
			1000	-18%	0.35
		GD & TKNC	100	2 %	0.9
			200	18%	0.43
			300	10%	0.70
			400	58%	0.003
			1000	-7%	0.73
		GD & SNAC	100	17 %	0.35
			200	11 %	0.62
			300	4 %	0.89
			400	-3 %	0.90
			1000	-14 %	0.47

Table 14: Correlation results between GD and coverage metrics using ResNet-20 and Cifar-10.

Dataset	Model	Metric	Test Set Size	Spearman	P-value
SVHN	LeNet-5	GD & LSC	100	15%	0.37
			200	27%	0.09
			300	2%	0.91
			400	15%	0.46
			1000	34%	0.06
		GD & DSC	100	-16 %	0.33
			200	9%	0.58
			300	19%	0.28
			400	14%	0.47
			1000	-14%	0.45
		GD & NC	100	-8%	0.61
			200	4%	0.79
			300	30%	0.08
			400	-28%	0.14
			1000	-12%	0.52
		GD & KMNC	100	44%	0.001
			200	66%	0.002
			300	23%	0.19
			400	-2%	0.9
			1000	46%	0.01
		GD & NBC	100	9%	0.58
			200	5%	0.77
			300	-19%	0.27
			400	26%	0.18
			1000	28%	0.12
		GD & TKNC	100	-3%	0.83
			200	1%	0.95
			300	-22%	0.20
			400	-15%	0.43
			1000	18%	0.34
		GD & SNAC	100	9%	0.58
			200	5%	0.77
			300	-19%	0.27
			400	26%	0.18
			1000	28%	0.12

Table 15: Correlation results between GD and coverage metrics using LeNet-5 and SVHN.